

Structural and synthetic insights into the chemistry of lithium tetraorganozincates

Andryj M. Borys^a, Marzia Dell'Aera^b, Vito Capriati^{b,*}, and Eva Hevia^{a,*}

^aDepartement für Chemie, Biochemie und Phamarzie, Universität Bern, Bern, Switzerland

^bDipartimento di Farmacia-Scienze del Farmaco, Università degli Studi di Bari "Aldo Moro", Consorzio C.I.N.M.P.I.S., Via E. Orabona 4, Bari, Italy

*Corresponding author: e-mail address: vito.capriati@uniba.it; eva.hevia@unibe.ch

Contents

1. Introduction and historical background	1
2. Synthesis and structural features of higher-order lithium zincates	3
2.1 Synthesis of lithium zincates	3
2.2 Synthesis and structural features of higher-order lithium zincates	6
2.3 Solution-state redistributions of lithium zincates	13
3. Applications in organic chemistry	17
3.1 Halogen (or tellurium)–zinc exchange, nucleophilic addition and substitution reactions	17
3.2 Deprotonative metalation and cross-coupling reactions	27
3.3 Polymerization reactions	29
4. Conclusions and outlook	33
Acknowledgments	35
References	35

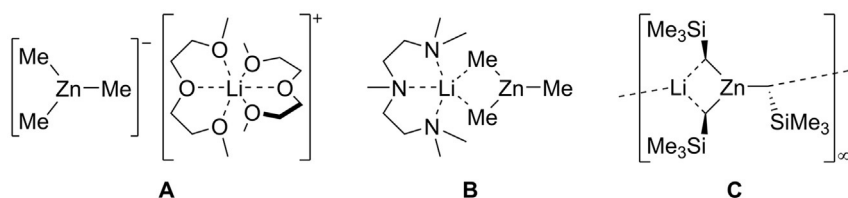


1. Introduction and historical background

Organozinc compounds, namely Et_2Zn and Me_2Zn , were reported by Edward Frankland in 1848 and represent the first known metal–alkyl and main–group organometallic compounds.^{1–3} Ten years later, J. Alfred Wanklyn documented the first organozincate, $[\text{Et}_3\text{ZnNa}]$, originally described as a “double compound between sodium–ethyl and zinc–ethyl.”⁴ It took a further 90 years until the first tetraorganozincate species, $[\text{Me}_4\text{ZnLi}_2]$, was synthesized by Dallas Hurd through the reaction of Me_2Zn with 2 equiv. of MeLi in Et_2O .⁵ The synthetic utility of organozincates was recognized shortly after by Georg Wittig, who coined the

term “ate” complexes to describe the special reactivity that these bimetallic compounds exhibited over their monometallic counterparts.⁶ Since then, organozincates have evolved from mere laboratory curiosities to versatile reagents in synthesis due to their unique reactivity and chemoselectivity in a range of organic transformations, including deprotonative metallation, metal-halogen exchange, and nucleophilic addition reactions.^{7–13} For example, the remarkable synergistic reactivity of organozincates is exemplified by $t\text{Bu}_4\text{ZnLi}_2$, which has been demonstrated to enable the zinc-halogen exchange and subsequent functionalisation of iodoarenes even in the presence of acidic functional groups such as alcohols; no reaction is observed with $t\text{Bu}_2\text{Zn}$ alone while $t\text{BuLi}$ gave a mixture of undesirable side-products.¹⁴

Recent advances in this field have been driven by a greater understanding on the constitution and the synthesis of these heterobimetallic reagents. These studies have revealed different stoichiometries regarding the Li:Zn ratio, with a myriad of structural motifs that span from solvent-separated ion species where lithium is solvated by an excess of solvent or a suitable Lewis donor, forming a discrete cation that does not interact with the zincate anion (i.e., $[\text{Me}_3\text{Zn}]^-[\text{Li}(\text{diglyme})_2]^+$ (**A**), Scheme 1)¹⁵ to contacted-ion pair structures that can be monomeric such as $\text{Me}_3\text{ZnLi}(\text{PMDETA})$ (**B**)¹⁵ (where PMDETA = N,N,N',N'',N''' -pentamethyldiethylenetriamine) or even oligomeric such as $[(\text{Me}_3\text{SiCH}_2)_3\text{ZnLi}]_\infty$ (**C**) which exhibits a complex 1D chain structural motif.¹⁶



Scheme 1 Examples of different structural motifs observed in lithium zincates.

Building on these developments, this chapter focusses on a particular type of lithium zincate, higher-order complexes with the empirical formulation R_4ZnLi_2 ($\text{R} = \text{alkyl, aryl, alkynyl, etc.}$). These hetero-tri-nuclear complexes have shown greater reactivity and kinetic activation than the relevant lower-order R_3ZnLi species, emerging as powerful and versatile reagents in organic synthesis. Herein we showcase a collection of representative examples focussing on the synthetic strategies to access these compounds, their key structural features, solution-state constitution and stability,

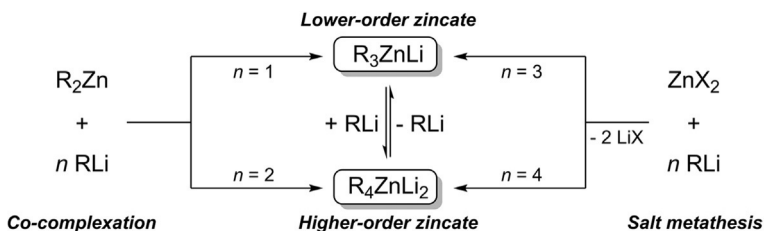
as well as their most relevant applications in organic synthesis. The main aim of this chapter is to provide a concise guide to advance the understanding on the close interplay of structural/reactivity correlations in this type of mixed-metal reagents, which enable their special synergistic reactivity and maximize chemical cooperativity between Li and Zn.



2. Synthesis and structural features of higher-order lithium zincates

2.1 Synthesis of lithium zincates

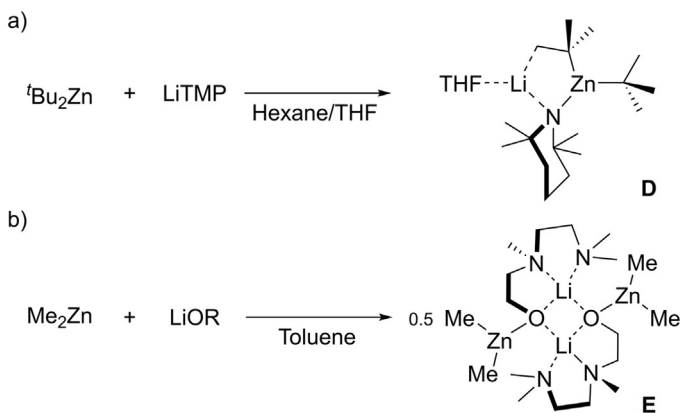
There are two primary methods that are frequently employed to access lithium zincates (Scheme 2).¹⁶ The first method involves co-complexation of a diorganozinc compound with an organolithium reagent. When the ratio of lithium to zinc is 1:1, a triorganozincate $[\text{R}_3\text{ZnLi}]$ is formed, which is classified as a lower-order zincate. When the ratio of lithium to zinc is 2:1, a tetraorganozincate $[\text{R}_4\text{ZnLi}_2]$ is formed, which is classified as a higher-order zincate. Higher-order zincates show enhanced reactivity compared to lower-order zincates due to greater kinetic activation of the formally dianionic zinc centre. The formation of lower- or higher-order zincates is influenced by a number of factors, including the nature of the anionic ligands and the identity of donor solvents or additives, and complex equilibria or redistribution processes have been reported and investigated for several lithium zincates (see Section 2.3). The second method to prepare lithium zincates involves salt metathesis of zinc salts (ZnX_2 , where X = halide or pseudohalide) with 3 or 4 equiv. of an organolithium reagent, to give either a lower- or a higher-order zincate, respectively.



Scheme 2 Synthesis of lower- and higher-order zincates *via* co-complexation or salt metathesis reactions.

The co-complexation method is generally favored since: (i) it avoids the formation of LiX salts, which often have to be separated from the reaction mixture; (ii) it can be conducted in non-donor solvents which enable precise

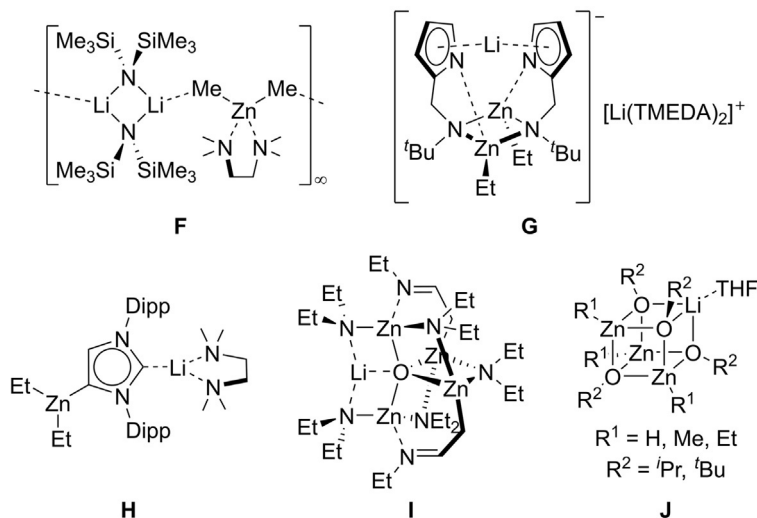
control over the presence of donor additives; and (iii) it allows the formation of heteroleptic lithium zincates by combining monometallic components bearing different R groups (Scheme 3).^{17–19}



Scheme 3 Examples of heteroleptic lithium zincates (**D**, **E**) obtained by the co-complexation of dialkylzinc reagents with (A) lithium amides or (B) alkoxides (TMP = 2,2,6,6-tetramethylpiperidide; R = $\text{CH}_2\text{CH}_2\text{N}(\text{Me})\text{CH}_2\text{CH}_2\text{NMe}_2$).

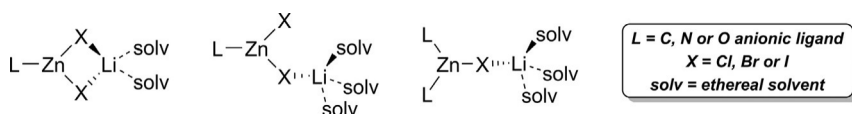
Several examples of lithium zincates adopting unique structural motifs or Li:Zn ratios differing from 1:1 or 2:1 have been reported (Scheme 4).^{20,21,22–29,30–35} The co-complexation of Me_2Zn with $\text{LiN}(\text{SiMe}_3)_2$ in the presence of TMEDA, for example, affords “inverse zincate” **F**,²⁴ while lithium zincate **G** derived from a bidentate amino-pyrrolyl ligand is a mixed contact-ion/solvent-separated species in which one Li^+ is sandwiched between the two pyrrolyl units.²⁸ Treatment of Et_2Zn with a C4-lithiated *N*-heterocyclic carbene affords the corresponding lower-order zincate **H** in which the Li^+ cation is solvated by the C2 carbene carbon and TMEDA; under different reaction conditions the carbene can instead coordinate to a second molecule of Et_2Zn which forces the Li^+ cation to be solvent-separated.³¹ Attempts to prepare $(\text{Et}_2\text{N})_2\text{Zn}$ *via* salt-metathesis of ZnCl_2 with Et_2NLi unexpectedly affords the lithium tetra-zinc species **I** in which an oxo ligand is encapsulated and coordinated to all five metal centres.²¹ A number of different zinc/lithium alkoxide cubanes **J** have been prepared through the treatment of dialkylzinc species with lithium alkoxides in the presence of water or

excess alcohol;²² alternatively, the tetrameric $[\text{HZnO}^t\text{Bu}]_4$ can be treated with various equivalents of LiO^tBu to give cubanes with different Zn:Li ratios including 3:1 (such as **J**), or 2:2 and 1:3.²⁹



Scheme 4 Examples of lithium zincates bearing non-traditional motifs and Li:Zn ratios.

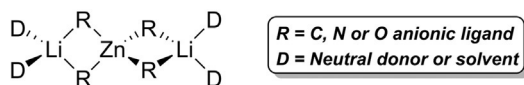
Numerous examples of organozinc compounds in which LiX ($\text{X} = \text{Cl}$, B or I) is retained within the structure following a salt–metathesis reaction between a lithiated ligand and ZnX_2 have been documented.^{36,37,38,39–45,46–55,56,57} These generally adopt one of three motifs depending on the nature of the anionic ligand and coordinating ethereal solvent (Scheme 5). Akin to Turbo–Grignard reagents^{58,59} or Turbo–Hauser bases⁶⁰ in which the addition of LiCl to RMgCl species (where $\text{R} = \text{alkyl}$ or amido) dramatically enhances the reactivity and/or selectivity, the presence or addition of LiX salts to organozinc reagents has been shown to play a similar role in various synthetic applications^{61–63} (most notably in Negishi cross-couplings)⁶⁴ as well as in the preparation of organozinc reagents themselves directly from organic halides and Zn metal.^{65–68} For specific details on the role of salt additives in organozinc chemistry, readers are directed to a recent review by Organ.⁶²



Scheme 5 Structural motifs of organozincate compounds containing co-complexed LiX .

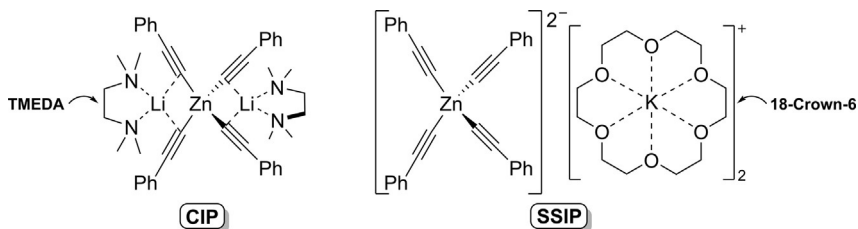
2.2 Synthesis and structural features of higher-order lithium zincates

Higher-order lithium zincates generally adopt the so-called Weiss motif (Scheme 6). This molecular assembly, which is common for alkali-metal “ate” complexes of tetrahedral divalent metals such as Mg or Zn,⁶⁹ was pioneered through ground-breaking structural studies by Erwin Weiss.⁷⁰ In this motif, the alkali-metal (lithium) and divalent metal (zinc) remain in close proximity, adopting in most case a *pseudo*-linear disposition, with the anionic ligands bridging between the two metals and the coordination-sphere of the alkali-metal being fulfilled by a suitable neutral donor or solvent. These contact-ion pairs (CIP), which may also be called contact-ion triples in the case of higher-order species, enable cooperativity between the two metal centres which are important for facilitating a range of stoichiometric^{10,71} and catalytic transformations.^{72,73}



Scheme 6 Graphical representation of the “Weiss motif” for higher-order lithium zincates.

Solvent-separated ions pairs (SSIP), or solvent-separated ion triples, are less common for higher-order alkali-metal “ate” complexes in comparison to lower-order species, since now a dianionic charge on the divalent metal must be delocalised onto the anionic ligands. For this reason, solvent-separated species are rarely encountered for higher-order species containing electron-rich alkyl, aryl, amide or alkoxide ligands, but are known for higher-order species containing electron-withdrawing ligands. For higher-order zincates, this includes cyanide⁷⁴ $[\text{Zn}(\text{CN})_4]^{2-}$ or fulminate⁷⁵ $[\text{Zn}(\text{CNO})_4]^{2-}$ complexes, but in these cases, they contain weakly coordinating ammonium cations or solvated Zn-dications, respectively, and not solvent-separated alkali-metal cations. The direct conversion from CIP to SSIP is known for some higher-order alkali-metal “ate” complexes through the addition of a suitable sequestering agents such as crown ethers or cryptands.⁷⁶ While this direct transformation is currently unknown for higher-order zincates, both contacted and solvent-separated structures have been independently reported for $[(\text{C}\equiv\text{C}-\text{Ph})_4\text{Zn}]^{2-}$: the former is a lithium zincate⁷⁷ adopting a “Weiss motif” and solvated by TMEDA (TMEDA = N, N, N', N'-tetramethylethylenediamine), while the latter is a potassium zincate⁷⁸ in which the K^+ cations are sequestered by 18-crown-6 (Scheme 7).



Scheme 7 Contacted and solvent-separated analogues of $[\text{Zn}(\text{C}\equiv\text{C-Ph})_4]^{2-}$.

The first and simplest tetraorganozincate species, $[\text{Me}_4\text{ZnLi}_2]$ (**1**) was prepared in 1948 through the co-complexation of Me_2Zn with 2 equiv. of MeLi in Et_2O .⁵ The unsolvated form, which is an ionic lattice, was structurally characterized by Weiss in 1968 through X-ray powder diffraction studies.⁷⁹ Two body-centred tetragonal space groups ($I\bar{4}$ and $I\bar{4}2m$) were considered which differ only in the positions of two of the four the Li atoms within the unit cell (Fig. 1). In both cases, the Zn atoms adopt distorted tetrahedral geometries with the four methyl substituents and feature short $\text{Li}\cdots\text{C}$ electrostatic interactions [2.515–2.836 or 2.483 Å].

The addition of donor solvents to polar organometallics is a well-established strategy to break down larger aggregates into smaller well-defined oligomers with improved solubility in hydrocarbon solvents.⁶⁹ This same phenomenon also applies to bimetallic “ate” complexes, and suitable donors are frequently added to enable their isolation, crystallization and solution-state characterization. In 2008, Hevia reported that the co-complexation of Me_2Zn with 2 equiv. of MeLi in the presence of bidentate amine donor TMEDA afforded the monomeric higher-order zincate, $[\text{Me}_4\text{ZnLi}_2(\text{TMEDA})_2]$ (**2**).⁸⁰ The solid-state structure shows a typical Weiss motif with a central Zn atom and neighboring Li atoms in tetrahedral environments (Fig. 2). The Zn—C bond lengths range from

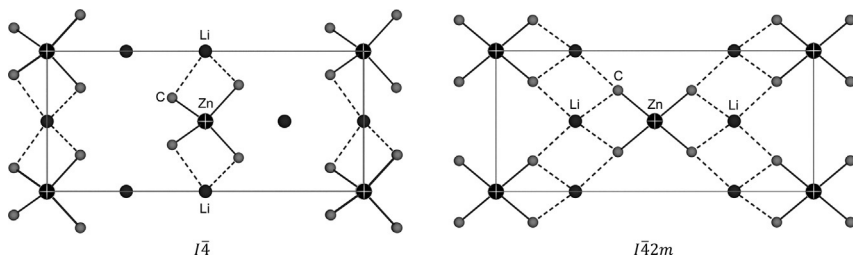


Fig. 1 Solid-state structure of $[\text{Me}_4\text{ZnLi}_2]$ (**1**) in two different body-centred tetragonal space groups, showing the unit cell along the crystallographic *b* axis.

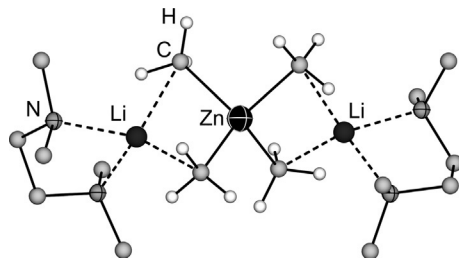


Fig. 2 Solid-state structure of $[\text{Me}_4\text{ZnLi}_2(\text{TMEDA})_2]$ (**2**). Hydrogen atoms on the TMEDA ligands are omitted for clarity.

2.118³ to 2.144³ Å, which are elongated relative to $\text{Me}_2\text{Zn}(\text{TMEDA})$ ⁸¹ [1.975⁸–1.990⁶ Å] and Me_2Zn ⁸² [1.91¹–1.92¹ Å]. Treating Me_2Zn with 1 equiv. of Me_2NLi surprisingly afforded the unsymmetrical mixed amido/alkyl tetraorganoazincate $[(\text{Me}_2\text{N})_3\text{MeZnLi}_2(\text{TMEDA})_2]$ (**3**) (see Section 2.3 for further details); this bears similar structural properties to **2**.⁸⁰

The same co-complexation approach with Et_2Zn and EtLi has been employed to access $[\text{Et}_4\text{ZnLi}_2]$, which can be crystallized with TMEDA (**4**) or the chiral bidentate amine donor (*R,R*)-TMCDA (TMCDA = *N,N,N',N'*-tetramethyl-1,2-diaminocyclohexane) (**5**); the latter represents the first structurally defined zincate with a chiral donor (Fig. 3).⁸³

For both $[\text{Me}_4\text{ZnLi}_2]$ and $[\text{Et}_4\text{ZnLi}_2]$, NMR spectroscopy can provide further insights into how the higher-order lithium zincates differ compared to the lower-order analogues or monometallic components.^{80,83} In $[\text{Me}_4\text{ZnLi}_2]$, the ¹H NMR signal of the methyl (CH_3) protons appears at $\delta -1.44$, which is upfield shifted with respect to $[\text{Me}_3\text{ZnLi}]$ ($\delta -1.08$) and Me_2Zn ($\delta -0.84$), and approaching that of MeLi ($\delta -1.96$). A similar

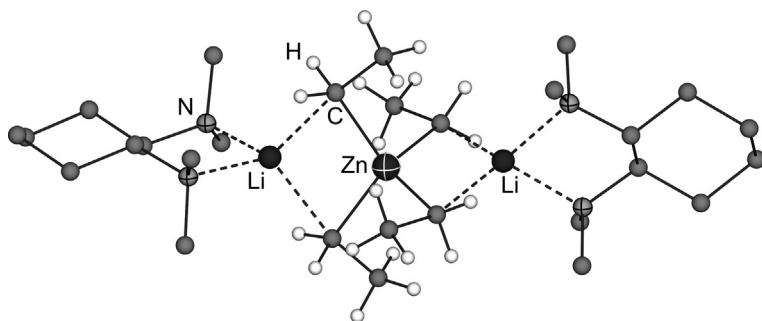
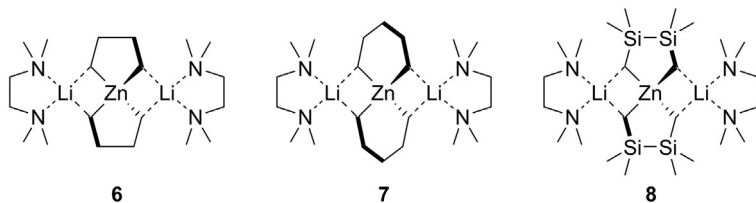


Fig. 3 Solid-state structure of $[\text{Et}_4\text{ZnLi}_2(\text{R,R})\text{-TMCDA}]_2$ (**5**). Hydrogen atoms on the (*R,R*)-TMCDA ligands are omitted for clarity.

trend is observed in the CH_2 signals of $[\text{Et}_4\text{ZnLi}_2]$ ($\delta -0.39$) relative to $[\text{Et}_3\text{ZnLi}]$ ($\delta -0.13$) and Et_2Zn ($\delta +0.11$). These observations are consistent with the increased nucleophilicity of higher-order zincates, which reflects their increased reactivity when compared to neutral diorganozinc compounds, while retaining the favorable selectivity in contrast to organolithium reagents.

Several examples of spirocyclic tetraorganozincates (**6–8**) have been documented and structurally characterized (Scheme 8).^{84–86} These compounds are prepared *via* a salt metathesis reaction between the corresponding dilithium compounds (prepared *in situ* from the alkyl-halide and Li metal) and ZnCl_2 . TMEDA has proven to be the favored donor to facilitate structural characterization by single crystal X-ray diffraction, but derivatives coordinated by etheral solvents such as Et_2O , THF and 1,4-dioxane have also been isolated. Differential thermal analysis (DTA) indicates that these spirocyclic derivatives show good thermal stability, ranging from 104 to 184 °C, which is highly dependent on the nature of the coordinated donor and alkyl ligands.^{84–86}



Scheme 8 Selected examples of spirocyclic tetraorganozincates.

Spirocyclic tetraorganozincates (**9–11**) derived from 1,4-dilithio-1,3-butadienes have also been reported and represent the first examples of well-defined zincacyclopentadienes (Fig. 4).⁸⁷ The solid-state structures deviate from the classical Weiss motif observed in spirocyclic derivatives

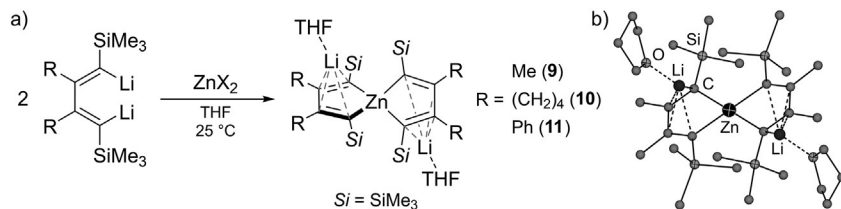


Fig. 4 (A) Synthesis of tetraorganozincates (**9–11**) derived from 1,4-dilithio-1,3-butadienes; (B) Solid-state structure of **9**. Hydrogen atoms omitted for clarity.

6–8; the central Zn atom still adopts a tetrahedral environment while the Li cations coordinate in a η^4 -fashion to the dianionic butadiene ligands with the final coordination site fulfilled by a molecule of THF. These compounds react with a further 0.5 equiv. of ZnX_2 ($\text{X}=\text{Cl}, \text{Br}$) to give 10-membered dizincacycles, or with S_8 or Se_8 to give the corresponding thiophenes or selenophenes.⁸⁷

The first structurally characterized tetraarylzincate $[\text{Ar}_4\text{ZnLi}_2]$ (where $\text{Ar}=\text{C}_6\text{H}_4\text{—CH}_2\text{NMe}_2$) (**12**) was reported in 1997;⁸⁸ this was prepared by the co-complexation of the corresponding aryl lithium and diarylzinc reagents in a 2:1 ratio. Unlike many “ate” complexes in which an external donor is required to solvate the alkali metal cation(s), the *ortho*- CH_2NMe_2 substituents on the aryl rings in **12** provide intramolecular coordination to the Li cations (Fig. 5). The solid-state structure reveals a typical Weiss motif with a slightly distorted tetrahedral environment at Zn; the Li cations also feature interactions with the two *ipso*-carbons to complete their coordination sphere. This molecular structure was found to be preserved in arene solution according to cryoscopic molecular weight determination and variable temperature NMR spectroscopy studies. Notably, two singlets between 210 and 330 K are observed in the ^1H NMR spectrum for the NMe_2 substituents; these coalesce upon heating to 346 K, indicating a fast $\text{N}\cdots\text{Li}$ dissociation/association process with an experimentally determined ΔG of 75.9 kJ mol^{-1} .⁸⁸

Intramolecular coordination has also been observed in tetraarylzincates derived from *ortho*-metalated anisole $[(\text{C}_6\text{H}_4\text{—OMe})_4\text{ZnLi}_2(\text{THF})_2]$ (**13**).⁸⁹ This compound forms through the disproportionation of the heteroleptic

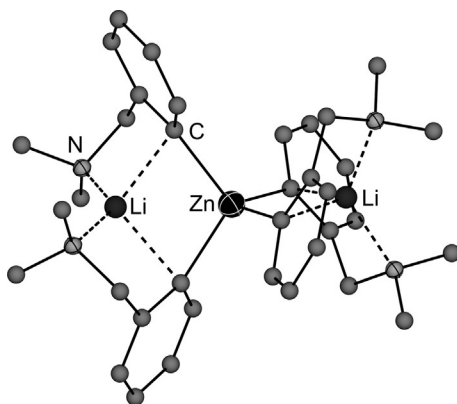


Fig. 5 Solid-state structure of **12**. Hydrogen atoms omitted for clarity.

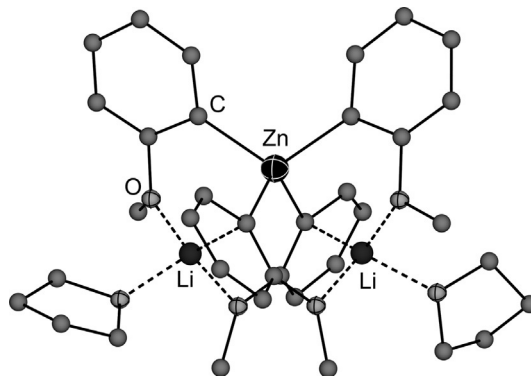


Fig. 6 Solid-state structure of **13**. Hydrogen atoms omitted for clarity.

triorganozincate $[(C_6H_4-OMe)Me_2ZnLi(THF)_2]$ (see Section 2.3 for further details). The solid-state structure of **13** does not exhibit a Weiss motif—instead the Li cations coordinate to three oxygen atoms (two from the OMe substituents and one from THF) and only one *ipso*-carbon (Fig. 6). This results in a $Li\cdots Zn\cdots Li$ vector of $91.09(15)^\circ$ which contrasts with the typical near-linear $Li\cdots Zn\cdots Li$ arrangement seen in other tetraorganozincates such as **12**.⁸⁸

The simplest tetraarylzincate $[Ph_4ZnLi_2]$ (**14**) has been prepared and fully characterized by multinuclear magnetic resonance spectroscopy,⁹⁰ but it has not yet been structurally elucidated as a discrete molecular compound. In 2016, Hevia reported that the co-complexation of PhLi with equimolar $(Me_3SiCH_2)_2Zn$ in benzene solution affords the heteroleptic species $[Ph_5(Me_3SiCH_2)_5Zn_3Li_4]_\infty$ (**15**).⁹¹ This can be envisaged as a three-component co-complex comprising of $[(Me_3SiCH_2)_3ZnLi]$, $[(Me_3SiCH_2)_2PhZnLi]$ and $[Ph_4ZnLi_2]$ —these dimerise in a head-to-tail fashion to give a cyclic 6-unit structure (Fig. 7), which further propagates into a polymeric 2D lattice *via* $Li\cdots\pi$ -arene interactions.

In the $[Ph_4ZnLi_2]$ unit (Fig. 8), the Zn centre adopts a distorted tetrahedral geometry; three Li cations interact with the *ipso*-carbons of the three phenyl substituents on Zn—these three Li cations and *ipso*-carbons lie in an approximate plane ~ 0.82 Å below Zn. The coordination of each Li cation is further fulfilled by additional interactions to CH_2SiMe_3 or Ph substituents on a neighboring lower-order zincate, as seen in Fig. 7.⁹¹ The structural diversity observed for $[Ar_4ZnLi_2]$ systems,^{88,89,91} where $Ar = Ph, 2-OMe-C_6H_4$ or $2-CH_2NMe_2-C_6H_4$, illustrates how the presence and identity of internal or external donors dramatically dictates the Li coordination, and thus overall solid-state structure.

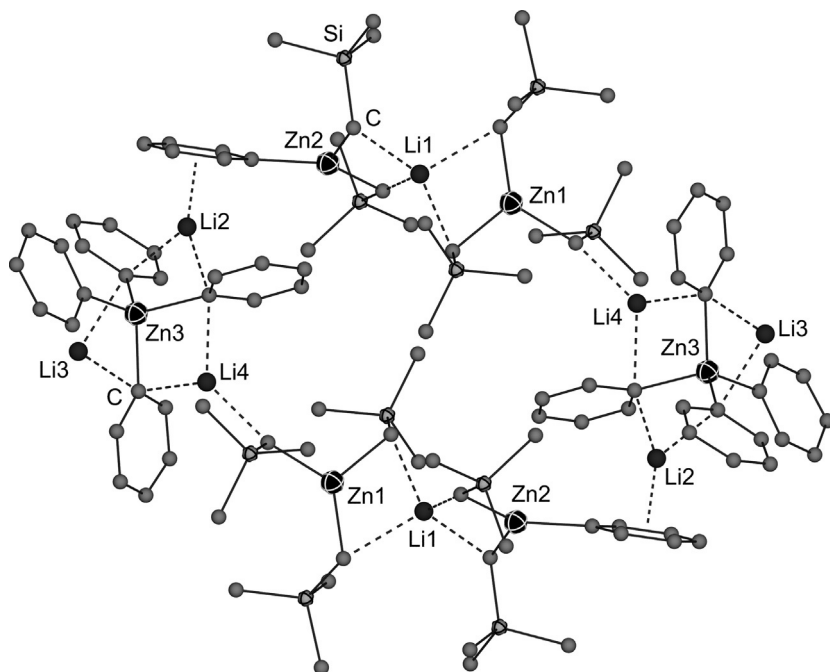


Fig. 7 Solid-state structure of **15**. Hydrogen atoms omitted for clarity.

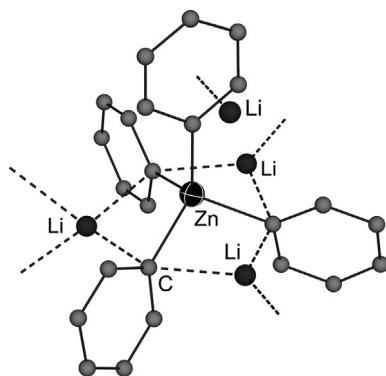


Fig. 8 Simplified view of the $[\text{Ph}_4\text{ZnLi}_2]$ unit in **15**. Hydrogen atoms omitted for clarity.

Tetraorganozincates bearing *sp*-hybridized carbon substituents, $[(\text{Ph}-\text{C}\equiv\text{C})_4\text{ZnLi}_2(\text{TMEDA})]$ (**16**), have also been prepared and structurally characterized.⁷⁷ Unlike the typical salt-metathesis routes, which employ ZnX_2 ($\text{X} = \text{Cl}$ or Br) as the zinc source, compound **16** was prepared using a halide-free method through treatment of $\{(\text{Me}_3\text{Si})_2\text{N}\}_2\text{Zn}$

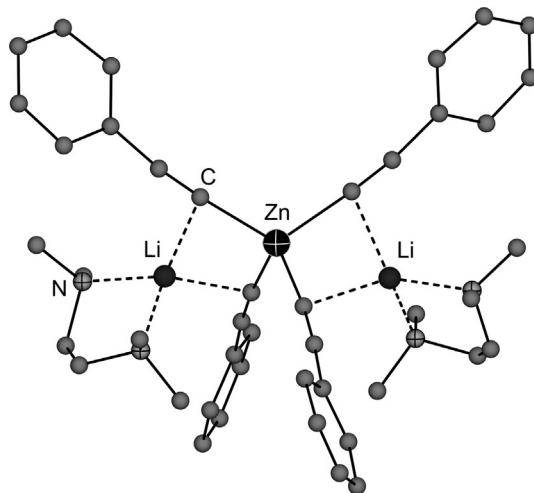


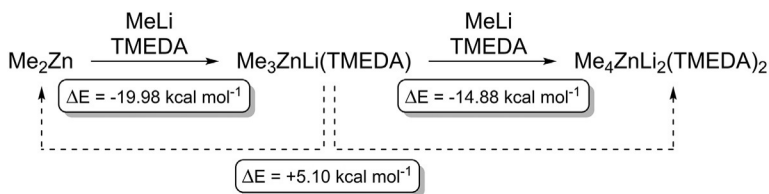
Fig. 9 Solid-state structure of **16**. Hydrogen atoms omitted for clarity.

with 4 equiv. of $\text{Ph}-\text{C}\equiv\text{C}-\text{Li}$, with liberation of 2 equiv. of $(\text{Me}_3\text{Si})_2\text{NLi}$ as the by-product. The solid-state structure of **16** adopts a typical Weiss motif where the TMEDA-solvated Li cations interact with two acetylide carbons (Fig. 9). This well-defined monomeric structure differs to the polymeric structures observed in tetraethynylzincates^{92,93} $[(\text{H}-\text{C}\equiv\text{C})_4\text{ZnAM}_2]_\infty$ bearing heavier alkali-metals such as K or Rb; polymeric arrangements have also been observed in related higher-order magnesiates bearing Na cations.⁹⁴ For heavier alkali-metals beyond Li, η^2 -coordination to the acetylide π -system is observed in contrast to the η^1 -coordination in **16**.⁷⁷

2.3 Solution-state redistributions of lithium zincates

Complex solution-state redistribution processes between lower-order and higher-order species have been documented and investigated for several different lithium zincates. In 1999, Berger used ^{13}C -labelling studies and NMR spectroscopy to investigate the co-complexation of Me_2Zn and MeLi in THF solution.⁹⁵ The lower-order zincate $[\text{Me}_3\text{ZnLi}]$ was found to form readily while the addition of a second equiv. of MeLi did not completely form the higher-order species $[\text{Me}_4\text{ZnLi}_2]$, but instead resulted in an equilibrium $[\text{Me}_3\text{ZnLi}] + \text{MeLi} \rightleftharpoons [\text{Me}_4\text{ZnLi}_2]$ which was observed to lie to the left-hand side. This behavior contrasts with studies by Hevia in 2008 in which the co-complexation of Me_2Zn and MeLi was performed in toluene in the presence of TMEDA.⁸⁰ Here it was found that the higher-order

species $[\text{Me}_4\text{ZnLi}_2(\text{TMEDA})_2]$ (**2**) forms regardless of the stoichiometry, suggesting that the lower-order species $[\text{Me}_3\text{ZnLi}(\text{TMEDA})]$ may exist in equilibrium with **2** and Me_2Zn . DFT calculations indicate that the formation of the lower-order species $[\text{Me}_3\text{ZnLi}(\text{TMEDA})]$ is thermodynamically favored by $-19.98 \text{ kcal mol}^{-1}$ with respect to the monometallic components; the tetraorganozincate $[\text{Me}_4\text{ZnLi}_2(\text{TMEDA})_2]$, however, is further energetically favored by $-14.88 \text{ kcal mol}^{-1}$ upon addition of MeLi and TMEDA (Scheme 9). The redistribution of $[\text{Me}_3\text{ZnLi}(\text{TMEDA})]$ to $[\text{Me}_4\text{ZnLi}_2(\text{TMEDA})_2]$ and Me_2Zn was found to be endothermic by $+5.10 \text{ kcal mol}^{-1}$, suggesting that this process is unfavorable in the gas-phase. Since this differs from experimental findings, it was proposed that the formation of solvent-separated species may account for this behavior and the contrasting observations in bulk THF⁹⁵ vs with TMEDA .⁸⁰



Scheme 9 Co-complexation and redistribution processes of Me_2Zn and MeLi according to DFT calculations.

Further support for this hypothesis can be seen through NMR and DFT studies carried out by Uchiyama on $[\text{tBu}_3\text{ZnLi}]$ which indicate a favorable redistribution process into $[\text{tBu}_4\text{ZnLi}_2]$ and tBu_2Zn in THF solution.⁹⁶ Specifically, the addition of 1 equiv. of tBuLi to tBu_2Zn in THF gives a mixture of $[\text{tBu}_4\text{ZnLi}_2]$ and tBu_2Zn with no spectroscopic evidence of $[\text{tBu}_3\text{ZnLi}]$. Computationally, the formation of $[\text{tBu}_3\text{ZnLi}]$ was found to be favorable by $-4.8 \text{ kcal mol}^{-1}$ with respect to the monometallic species, however, the higher-order zincate $[\text{tBu}_4\text{ZnLi}_2]$ forms upon further addition on tBuLi with additional $-11.7 \text{ kcal mol}^{-1}$ stabilization. The redistribution of two molecules of $[\text{tBu}_3\text{ZnLi}]$ into $[\text{tBu}_4\text{ZnLi}_2]$ and tBu_2Zn is thermodynamically favored by $-6.9 \text{ kcal mol}^{-1}$, in support of experimental findings.⁹⁶ Despite these results, the lower-order zincate can be trapped by a *N*-heterocyclic carbene (NHC); 1,3-bis(2,6-di-isopropylphenylimidazol-2-ylidene) to give $\text{tBu}_3\text{ZnLi}(\text{NHC})$ (Fig. 10), illustrating the crucial role of the Lewis donor and/or solvent in the stabilization of these heterobimetallic complexes.⁹⁷

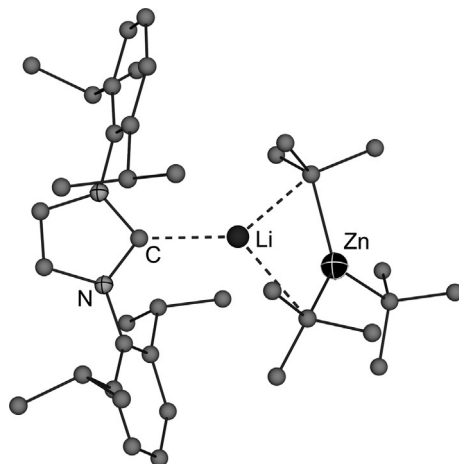
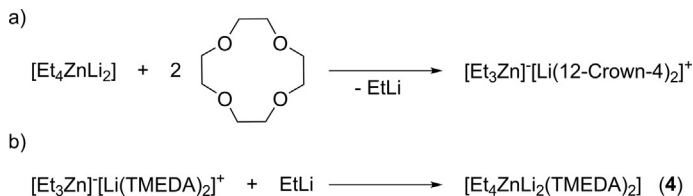


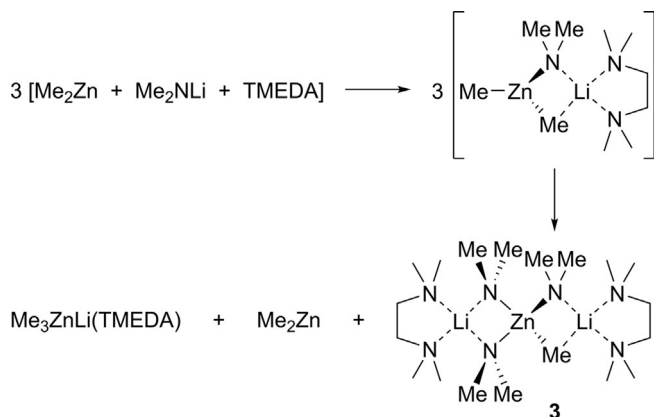
Fig. 10 Solid-state structure of ${}^t\text{Bu}_3\text{ZnLi}(\text{NHC})$. Hydrogen atoms omitted for clarity.

For $[\text{Et}_4\text{ZnLi}_2]$, it was again found that no redistribution to $[\text{Et}_3\text{ZnLi}]$ and EtLi was observed in toluene solution.⁸³ Contrastingly, the addition of 2 equiv. of 12-crown-4 to $[\text{Et}_4\text{ZnLi}_2]$ results in a disproportionation to the lower-order solvent-separated zincate $[\text{Et}_3\text{Zn}]^-[\text{Li}(12\text{-crown-4})_2]^+$ and EtLi (Scheme 10A). On the other hand, treating the analogous TMEDA solvate $[\text{Et}_3\text{Zn}]^-[\text{Li}(\text{TMEDA})_2]^+$ with EtLi forms the higher-order contacted species $[\text{Et}_4\text{ZnLi}_2(\text{TMEDA})_2]$ (**4**) (Scheme 10B), demonstrating that these redistribution processes can be manipulated by the choice of donor.⁸³ These results further suggest that the formation of solvent-separated species plays a key role in these processes, such that lower-order species may favor solvent-separated ion pairs while higher-order species adopt contacted structures in both solution and the solid-state.



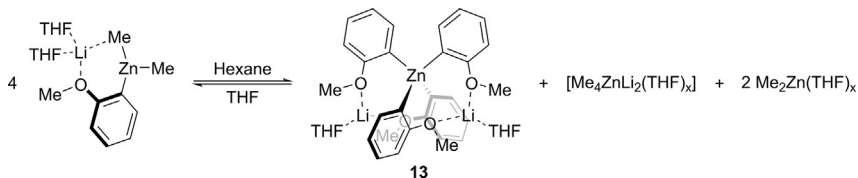
Scheme 10 Redistribution processes of higher- (A) and lower-order lithium zincates (B) derived from Et_2Zn and EtLi .

Further complexity in these redistribution processes is observed for heteroleptic tetraorganozincate derivatives. The mixed amido/alkyl species $[(\text{Me}_2\text{N})_3\text{MeZnLi}_2(\text{TMEDA})_2]$ (**3**) unexpectedly forms when treating Me_2Zn with equimolar Me_2NLi and TMEDA.⁸⁰ Here, it is proposed that the heteroleptic lower-order species $[(\text{Me}_2\text{N})\text{Me}_2\text{ZnLi}(\text{TMEDA})]$ which initially forms, then rearranges to give **3** alongside $[\text{Me}_3\text{ZnLi}(\text{TMEDA})]$ and Me_2Zn , as supported by NMR spectroscopy (Scheme 11). Attempts to prepare the homoleptic tetraamidozincate $[(\text{Me}_2\text{N})_4\text{ZnLi}_2(\text{TMEDA})_2]$ by treating ZnCl_2 with 4 equiv. of Me_2NLi failed, and only the lower-order variant $[(\text{Me}_2\text{N})_3\text{ZnLi}(\text{TMEDA})]_2$ could be isolated. The favorable formation of this species was attributed to its lower solubility in hexane which results in its selective crystallization. $[(\text{Me}_2\text{N})_3\text{ZnLi}(\text{TMEDA})]_2$ was nevertheless found to exist in equilibrium with $[(\text{Me}_2\text{N})_4\text{ZnLi}_2(\text{TMEDA})_2]$ and $(\text{Me}_2\text{N})_2\text{Zn}$ when dissolved in benzene, and this can be pushed toward the higher-order species through addition of Me_2NLi .⁸⁰



Scheme 11 Formation of higher-order mixed amide/alkyl zincate **3** through redistribution of a proposed lower-order species.

Similar redistribution processes have also been observed in aryl-substituted zincates. While the structure of the higher-order tetraarylzincate $[\text{Ar}_4\text{ZnLi}_2]$ (where $\text{Ar} = \text{C}_6\text{H}_4\text{—CH}_2\text{NMe}_2$) (**12**) was found to be retained in toluene solution, the lower-order analogue $[\text{Ar}_3\text{ZnLi}]$ exists in equilibrium with **12** and Ar_2Zn , but is favored at low temperatures.⁸⁸ Although not involving higher-order zincates, it was found that attempts to prepare heteroleptic derivatives through the co-complexation of Ar_2Zn with $\text{Me}_3\text{SiCH}_2\text{Li}$ instead favors the respective homoleptic zincates $[\text{Ar}_3\text{ZnLi}]$ and $[(\text{Me}_3\text{SiCH}_2)_3\text{ZnLi}]$.



Scheme 12 Solvent-induced formation of $[(\text{C}_6\text{H}_4\text{-OMe})_4\text{ZnLi}_2(\text{THF})_2]$ (**13**) from the heteroleptic triorganozincate $[(\text{C}_6\text{H}_4\text{-OMe})\text{Me}_2\text{ZnLi}(\text{THF})_2]$.

The preferential formation of homoleptic species was found to be responsible for the isolation of the related tetraarylzincate $[(\text{C}_6\text{H}_4\text{-OMe})_4\text{ZnLi}_2(\text{THF})_2]$ (**13**).⁸⁹ This compound reversibly forms through a solvent-induced disproportionation of the heteroleptic triorganozincate $[(\text{C}_6\text{H}_4\text{-OMe})\text{Me}_2\text{ZnLi}(\text{THF})_2]$ to give **13** alongside $[\text{Me}_4\text{ZnLi}_2(\text{THF})_x]$ and 2 equiv. of $\text{Me}_2\text{Zn}(\text{THF})_x$ (Scheme 12). The heteroleptic species was found to be stable in THF solution, while the addition of hexane results in the immediate precipitation of **13**. This process is reversible, however, and redissolution of **13** in THF with $[\text{Me}_4\text{ZnLi}_2(\text{THF})_x]$ and $\text{Me}_2\text{Zn}(\text{THF})_x$ regenerates $[(\text{C}_6\text{H}_4\text{-OMe})\text{Me}_2\text{ZnLi}(\text{THF})_2]$.

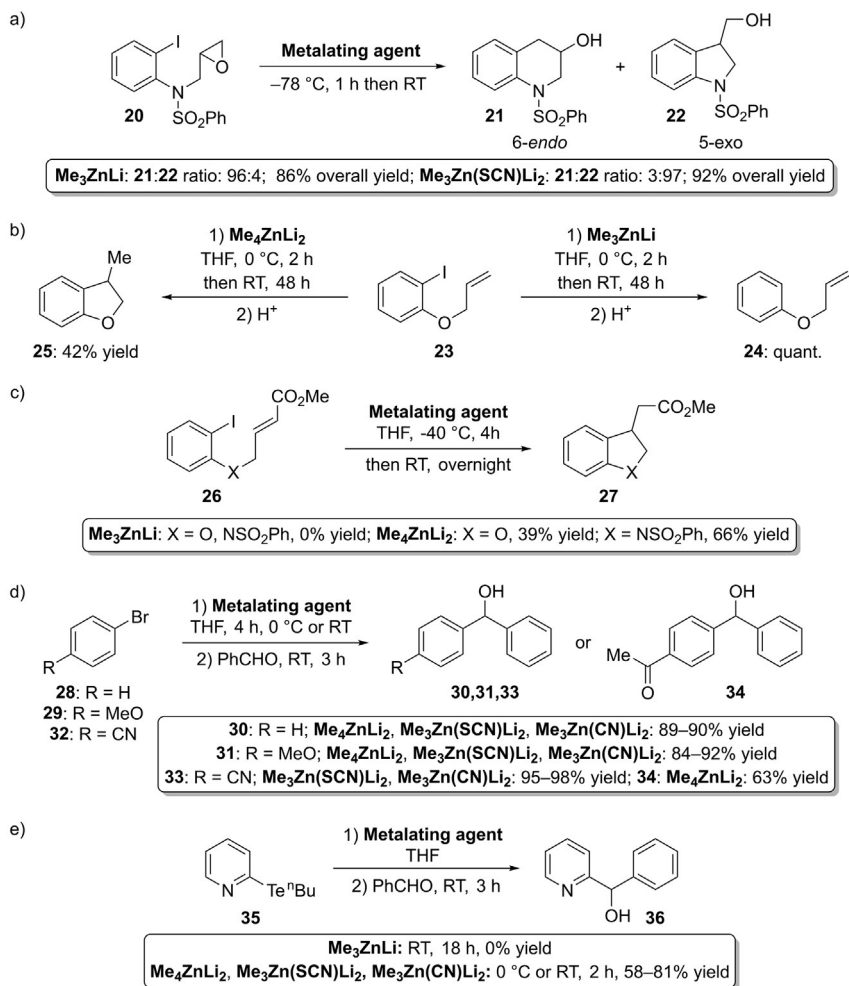


3. Applications in organic chemistry

In this section, we discuss the unique reactivity exhibited by *ad hoc* designed higher-order lithium zincates $[\text{R}_4\text{ZnLi}_2]$, which are bimetallic “ate” complexes usually arising from lithium triorganozincates $[\text{R}_3\text{ZnLi}]$ having Lewis acidity and organolithiums $[\text{RLi}]$ (or other lithium salts in the case of heteroleptic complexes) possessing Lewis basicity (see Section 2.1), toward nucleophilic addition and substitution, halogen (or tellurium)–zinc exchange, deprotonative metalation, cross-coupling and polymerization reactions. Comparison of the different reactivities and selectivities (if any) of tri- and tetraorganozincates in organic transformations will be provided as well.

3.1 Halogen (or tellurium)–zinc exchange, nucleophilic addition and substitution reactions

The regioselectivity of epoxide ring-opening reactions promoted by bimetallic complexes was first investigated by Uchiyama, Kondo and Sakamoto through variation of the nature of the organometallic reagent. When styrene oxide (**17**) was reacted in THF at room temperature (RT) with either Me_3ZnLi or Me_4ZnLi_2 , the two isomeric products **18** and **19** formed in almost equal amounts, albeit in different yields (Me_3ZnLi : 70%;

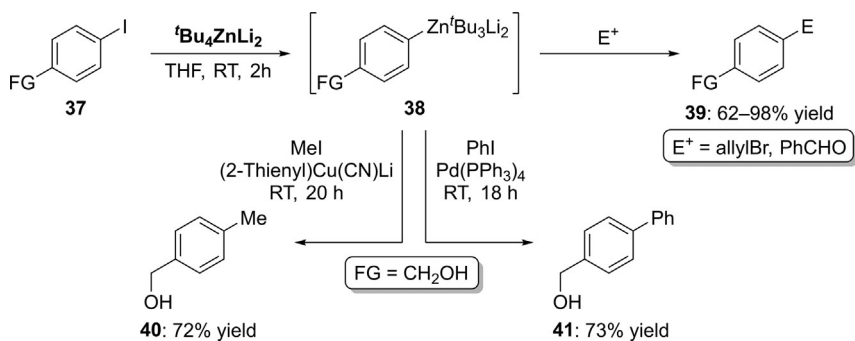


Scheme 14 Comparison of the reactivity of triorgano- and tetraorganozincates toward: (A) nucleophilic substitution; (B) intramolecular carbozincation; (C) intramolecular Michael addition; (D) halogen-zinc exchange; and (E) tellurium-zinc exchange. RT = room temperature.

Me₃Zn(CN)Li₂, which furnished product **33** as the sole product in up to 98% yield, whereas Me₄ZnLi₂, acting as both a metalating agent and nucleophile, gave 4-acetylbenzhydrol (**34**) in 63% yield upon hydrolysis (Scheme 14D).⁷ The tellurium-zinc exchange of 2-pyridinyltellurium compound **35** proceeds smoothly only with higher-order zincates. The corresponding putative 2-pyridinyl zincates could be trapped with

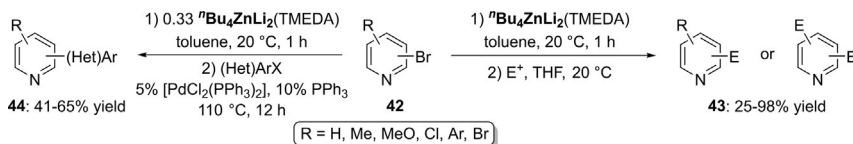
PhCHO to give compound **36** in 58–81% yield within 2 h at 0 °C or at RT. Under the same conditions, the reaction of **35** with Me₃ZnLi did not proceed at all even after 18 h at RT (Scheme 14E).⁷

A highly chemoselective protocol for the halogen–zinc exchange of functionalized aromatic derivatives was established by Uchiyama. Under mild and operationally simple conditions (0 °C, THF), a variety of substrates **37** containing acidic protons (amide N–H, phenolic O–H, glycerol C2–O–H), protected alcohols, Me₃Si-protected alkynes, an ester or amide, underwent smooth iodine–zinc exchange with ^tBu₄ZnLi₂ within 30 min. The corresponding arylzincate intermediate **38** could be utilized as an aryl anion equivalent to give either **39** (62–98% yield), after quenching with allyl bromide or PhCHO, or the alkylated or phenylated products **40,41** (72–73% yield) *via* copper- or palladium-catalyzed C–C bond-forming processes (Scheme 15). Aniline derivatives, π -deficient heteroaromatic moieties, as well as aliphatic iodides and *ortho*- and *para*-substituted compounds proved also to be good substrates.^{14,96} Interestingly, by increasing the temperature to 60 °C, even the bromine–zinc exchange reaction of aryl bromides with ^tBu₄ZnLi₂ proceeded with no problems, and proved to be compatible with various functional groups such as a Me₃Si-protected acetylene, amides, π -deficient heteroaromatic scaffolds and triflates, with the exception of benzylic moieties.⁹⁶ Of note, the formation of the mixed-metal complex was a prerequisite for a successful metalation to take place as a stepwise treatment of **37**, first, with alkyllithiums, and then with zinc reagents was not effective.



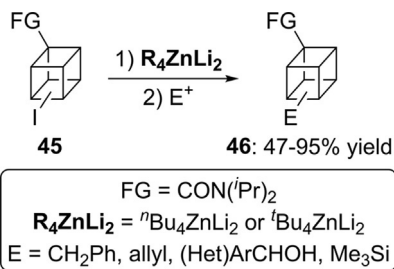
Scheme 15 Metalation of functionalized aryl iodides **37** and trapping of the zincated intermediates **38** with various electrophiles. FG=functional group. RT=room temperature.

Homoleptic tetraalkylzincates promote the efficient and chemoselective room-temperature bromine–metal exchange reactions of bromo- and dibromopyridines **42** in toluene to afford mono- and bifunctionalized derivatives **43** in moderate to excellent yields (from 25% to 98%) after quenching with electrophiles, by simply changing the ligand and the stoichiometry of the reagent.⁹⁹ The authors noted that the presence of TMEDA had a dramatic effect on the selectivity observed. Indeed, while ${}^n\text{Bu}_4\text{ZnLi}_2$ gave mainly monozincation, the use of ${}^n\text{Bu}_4\text{ZnLi}_2 \cdot \text{TMEDA}$ (1–2 equiv) favored dizincation. Palladium-catalyzed cross-coupling of zincated pyridines with (hetero)aryl halides were also feasible in toluene using ${}^n\text{Bu}_4\text{ZnLi}_2 \cdot \text{TMEDA}$ and provided compounds **44** in 41–65% yield (Scheme 16).⁹⁹



Scheme 16 Zincation of bromopyridines **42** and subsequent reactions with electrophiles or palladium-catalyzed cross-couplings with (hetero)aryl halides to give compounds **43** and **44**, respectively.

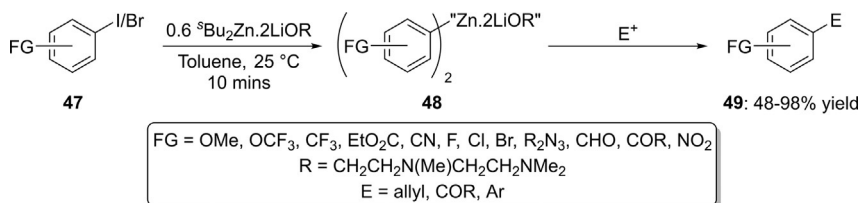
The practicability and synthetic utility of the iodine–metal exchange reaction was also examined with cubane using various lithium zincates. Polyfunctionalized cubane derivatives **46**, with potential utility as novel bioactive compounds, could be successfully prepared with reasonable yields (47–95%) and high selectivity by reacting 2- or 4-iodocubane-*N,N*-diisopropylcarboxamide **45** with dianionic zincates such as ${}^n\text{Bu}_4\text{ZnLi}_2$ or ${}^t\text{Bu}_4\text{ZnLi}_2$, followed by quenching with electrophiles, such as an organohalide or aldehyde (Scheme 17).¹⁰⁰ By contrast, the halogen–lithium



Scheme 17 Reaction of metalated cubanes, prepared from 2- or 4-iodocubane **45** and dianionic zincates R_4ZnLi_2 , with various electrophiles to give compounds **46**.

exchange led to cubyllithium species whose basicity was strong enough to cause undesirable protonation by any proton source present, or competitive side reactions. A recent review on the halogen–zinc exchange using tri- or tetraalkylzincates has been given by Knochel.¹⁰¹

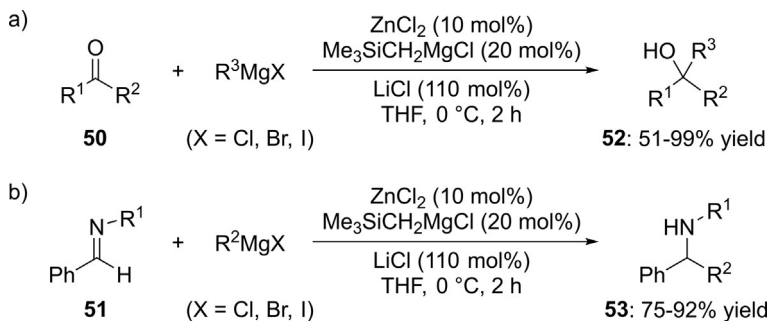
The heteroleptic higher-order lithium zincate ${}^s\text{Bu}_2\text{Zn}\cdot 2\text{LiOR}$ ($\text{R} = \text{CH}_2\text{CH}_2\text{N}(\text{Me})\text{CH}_2\text{CH}_2\text{NMe}_2$) was found to promote the efficient Zn/halogen (Br or I) exchange of a wide range of arenes and heteroarenes **47** in the presence of sensitive functional groups such as triazines, aldehydes and nitro substituents (Scheme 18).¹⁹ The polyfunctionalised diaryl- and diheteroaryl-zinc compounds **48** could then be quenched with various electrophiles *via* Cu-catalyzed allylation, Cu-mediated coupling with acyl chlorides, or Pd-catalyzed Negishi cross-coupling to give highly functionalized (hetero)arenes **49** in 48–98% yield. Multinuclear magnetic resonance spectroscopic studies including ${}^1\text{H}$ DOSY shed light on the constitution of the active species ${}^s\text{Bu}_2\text{Zn}\cdot 2\text{LiOR}$, indicating that it forms a contact-ion pair in toluene solution. This bimetallic species can be accessed by first treating Et_2Zn with 2 equiv. of the corresponding alcohol ROH, followed by 2 equiv. of ${}^s\text{BuLi}$, or by direct co-complexation of ${}^s\text{Bu}_2\text{Zn}$ with 2 equiv. of LiOR.¹⁹



Scheme 18 Zinc-halogen exchange of arenes and heteroarenes bearing sensitive functional groups using ${}^s\text{Bu}_2\text{Zn}\cdot 2\text{LiOR}$, and onward functionalisation with electrophiles.

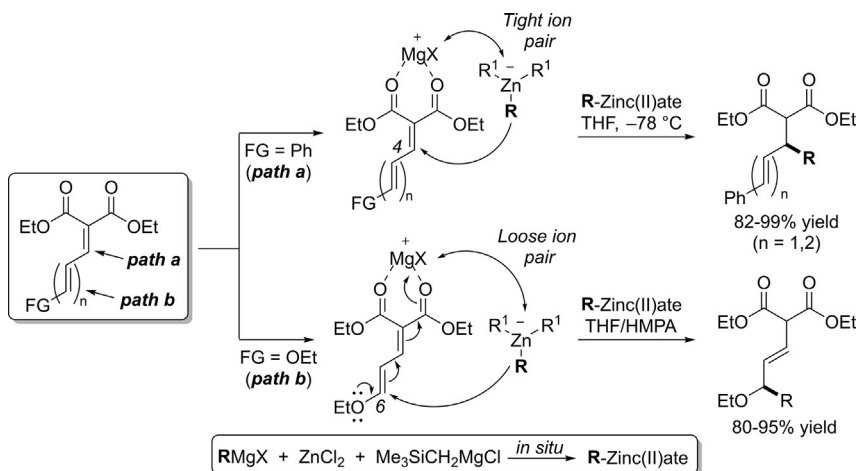
Highly efficient catalytic alkylation and arylation of ketones and aldehydes (**50**), and aldimines (**51**) have been achieved using Grignard reagents in the presence of ZnCl_2 , trimethylsilylmethyl magnesium chloride ($\text{Me}_3\text{SiCH}_2\text{MgCl}$) and LiCl. The reaction is thought to take place *via* the *in situ* formation of zincate $[\text{R}(\text{Me}_3\text{SiCH}_2)_2\text{Zn}][\text{Li}]^+[\text{MgX}_2]_m[\text{LiX}]_n$ (where X is typically Cl under the addition of LiCl) which acts as both a catalytic alkylating reagent displaying an enhanced nucleophilicity and also a Lewis acidic activator. Starting from a variety of commercially available Grignard reagents, this robust and reliable protocol allowed the isolation of the desired secondary or tertiary alcohols **52** and secondary amines **53** in high yields (up to 99%), while minimizing the

formation of side products by reduction *via* β -H transfer of Grignard reagents and/or competitive enolisation processes triggered by the strong basicity of Grignard reagents (Scheme 19).¹⁰²



Scheme 19 Addition of Grignard reagents to: (A) aldehydes and ketones; or to (B) imines, catalyzed by ZnCl_2 , $\text{Me}_3\text{SiCH}_2\text{MgCl}$, and LiCl .

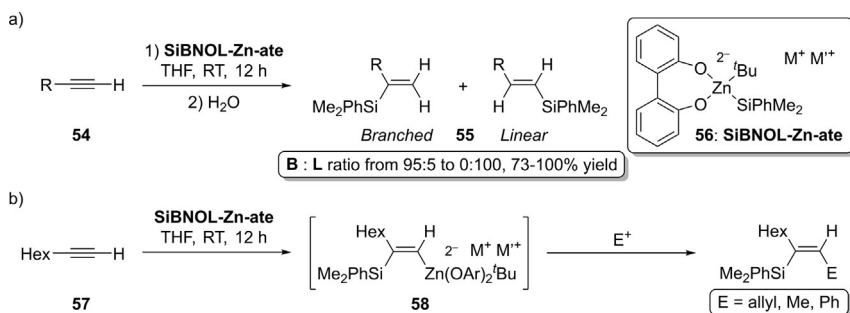
A transition-metal-free, highly regioselective 1,4- and 1,6-conjugate addition of Grignard reagent-derived organozincate complexes to malonate-derived polyconjugated esters was first developed by Ishihara.¹⁰³ Interestingly, the tight ion-pair between the cationic $[\text{MgX}]^+$ and the anionic $[\text{R}_3\text{Zn}]^-$ moiety, favored by chelation of the 1,3-dicarbonyl core to the Mg^+ center, promoted the 1,4-conjugate addition (Scheme 20, path a). On the other hand, the introduction



Scheme 20 Regioselective 1,4- and 1,6-conjugate additions (paths a and b) of Grignard reagent-derived organozincates to polyconjugated esters.

of an electron-donating group (EtO) to the substrate, with the use of HMPA, led to preferential 1,6-conjugate addition by weakening the aforementioned tight ion pair and selectively activating the terminal conjugate carbon atom at the 6-position (Scheme 20, path b).

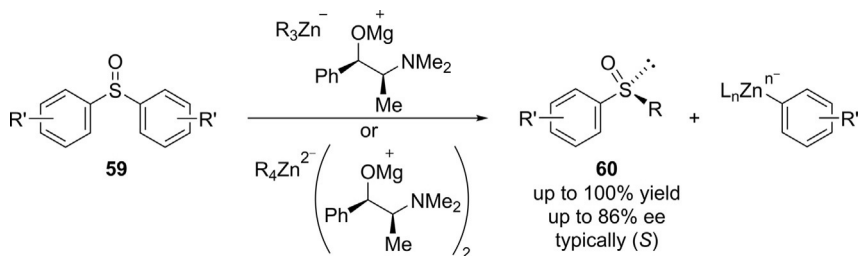
Dianionic silylzincate complexes promote the transition metal-free, highly chemo- and regioselective silylzincation of unfunctionalized and functionalized terminal alkynes **54**, thereby affording stereodefined trisubstituted olefins **55**, in good to excellent yields at room temperature, after aqueous quenching. Among various dianionic zincates examined, a combination of biphenoxo and ^tBu (SiBNOL-Zn-ate, **56**) gave the best results in terms of yield and functional group tolerance (Scheme 21A). As for regioselectivity, it was found that the reaction of SiBNOL-Zn-ate with terminal alkynes containing cyclic, alkyl, benzyl, and polar functional groups displayed branch selectivities. On the other hand, by enhancing the electrophilicity at the terminal carbon atom of alkynes, through the introduction of a Me₃Si, phenyl, or a pyridyl group, the production of linear products was favored over the branched ones. Of note, the putative dianionic vinylzincate intermediate **58**, *in situ* generated by silylzincation of 1-octyne (**57**) with **56**, could be successfully utilized as a vinyl anion equivalent, thereby providing regioselectively trisubstituted olefins, in high yields and selectivity, when reacted with allyl bromide or subjected to copper- or palladium-catalyzed C—C bond-forming reactions (Scheme 21B).¹⁰⁴



Scheme 21 (A) Silylzincation of various functionalized terminal alkynes. (B) Electrophilic trapping of the intermediate **58**, *in situ* generated by silylzincation of 1-octyne (**57**) using SiBNOL-Zn-ate complex. RT = room temperature.

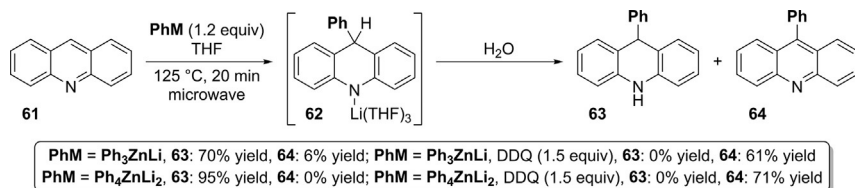
The first asymmetric sulfinylation of alkylzinc compounds was reported by Brückner and Ruppenthal in 2018.¹⁰⁵ Symmetric diarylsulfoxides **59** were

efficiently desymmetrised by reacting them with both tri- and tetraalkylzincates containing one or two enantiomerically pure (*S,S*)-configured β -amino (magnesiokoalkoxide) cations. When using *N*-methyl-($-$)-ephedrine as the ligand, THF as the solvent, and a temperature as low as $-78\text{ }^{\circ}\text{C}$, arylsulfonylation produced aryl alkyl sulfoxides **60** in up to quantitative yields and with ee values up to 86% (Scheme 22).



Scheme 22 Asymmetric arylsulfonylation using tri- and tetraorganozincates containing an *N*-methyl-($-$)-ephedrine-based magnesium β -aminoalkoxide as a chiral nonracemic counterion.

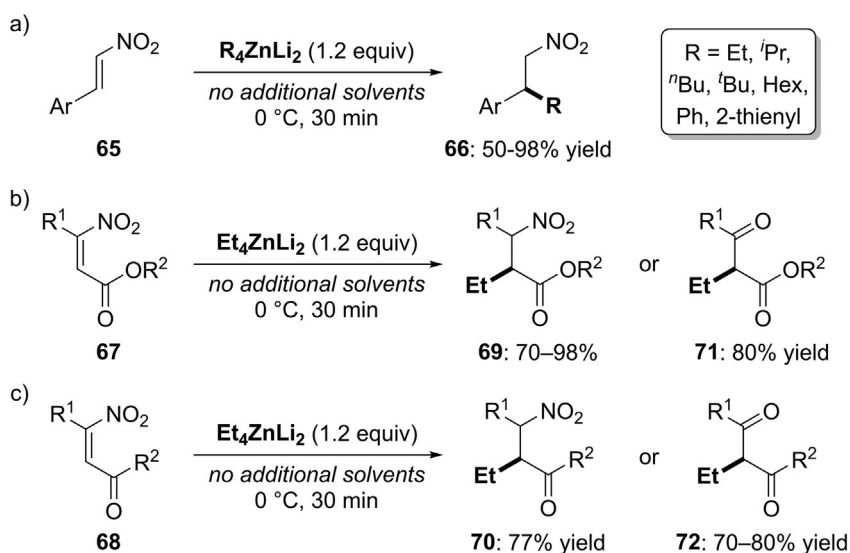
A transition-metal-free, direct C—H arylation of acridine (**61**), a representative electron-deficient *N*-heterocyclic molecule, has been thoroughly investigated by Hevia using homo(aryl) lithium zincates such as Ph_3ZnLi and Ph_4ZnLi_2 , which were readily prepared by co-complexation of variable amounts of their monometallic components (PhLi and Ph_2Zn).⁹⁰ Using microwave irradiation ($125\text{ }^{\circ}\text{C}$, 20 min), both zincates regioselectively transferred a Ph group to the 9 position of **61** to give mixtures of the arylated products **63** (70–95% yield) and **64** (up to 6% yield) *via* intermediate **62**, which was isolated and structurally and spectroscopically characterized (Scheme 23). Of note, Ph_2Zn was unable to transfer one of its phenyl groups to **61**, unless using a transition-metal catalyst and harsh conditions



Scheme 23 Transition-metal-free C9 arylation of acridine (**61**) using Ph_3ZnLi and Ph_4ZnLi_2 as nucleophiles, under microwave irradiation in THF, to give compounds **63** and **64** *via* intermediate **62**.

(130 °C, 20 h). Final oxidation of **63** with 2,3-dichloro-5,6-dicyano-1,4-benzoquinone (DDQ) provided **64** as the sole product in up to 71% yield (Scheme 23).¹¹ Radical addition pathways are thought to play a major role when alternatively using an excess of PhLi and TMEDA (3 equiv.).

Hevia and Capriati have recently reported the first transition-metal catalyst- and ligand-free application for the regioselective, conjugate addition of R_4ZnLi_2 species to nitroolefins **65**.⁸³ Displaying enhanced nucleophilicity compared to alkylzinc halides and dialkylzinc reagents, both homoleptic aliphatic and aromatic R_4ZnLi_2 species provided access to valuable nitroalkanes **66** in up to 98% yield with short reaction times (30 min), mild reaction conditions (0 °C), and with exceptional functional group tolerance (Scheme 24A). Of note, by performing such addition reactions under nitrogen and in the absence of additional solvents, compounds **66** were isolated as the sole products, with the notorious replacement of the vinylic nitro group by an alkyl group (often observed in the absence of a Lewis acid and in ethereal solvents) being totally suppressed. The synthetic scope of this protocol was successfully expanded to include β -nitroacrylates **67** (Scheme 24B) and β -nitroenones **68** (Scheme 24C), where despite the presence of other electrophilic groups, selective 1,4-addition to the carbon-carbon double bond proved to be preferred, with compounds **69** and **70** (in which either the ester

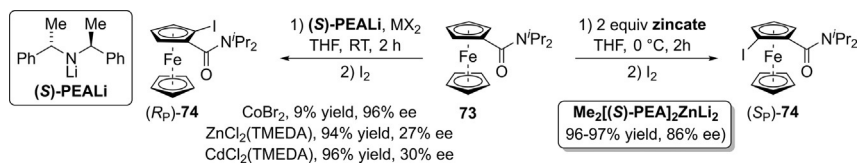


Scheme 24 Nucleophilic addition of tetraorganozincates R_4ZnLi_2 to: (A) nitroolefins **65**; (B) β -nitroacrylates **67**; and (C) β -nitroenones **68** to give products **66** and **69–72**.

or the carbonyl moiety remained untouched) forming in 70–98% yield. For some derivatives, spontaneous hydrolysis of the nitro group (Nef reaction) was also found to take place during the work-up procedure, thus furnishing β -ketoesters and β -diketones **71** and **72** in 70–80% yield. Structural and spectroscopic studies (i) confirmed the dianionic nature of the zincate and probed the constitution of these bimetallic reagents, thus strongly supporting the formation of highly nucleophilic lithium tetraorganozincates in solution, and (ii) unveiled the influence that donor additives can have on both the structure and aggregation of these reagents, with chelating diamine TMEDA and (*R,R*)-TMCDA favoring contacted ion species, while macrocyclic Lewis donor (12-crown-4) promoted a disproportionation process to the solvent-separated R_3ZnLi species and RLi (see Sections 2.2 and 2.3 for further details).

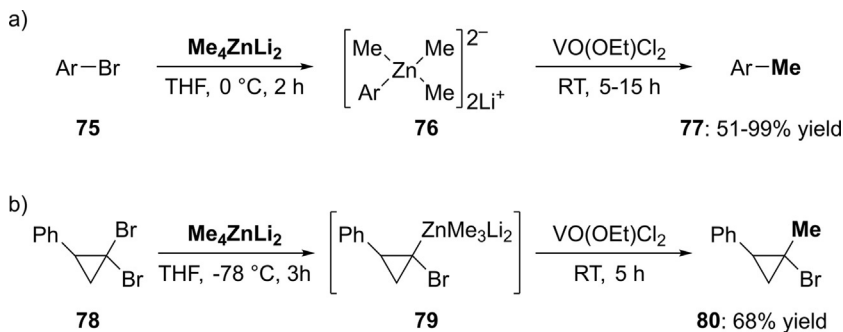
3.2 Deprotonative metalation and cross-coupling reactions

The stereoselective synthesis of chiral 1,2-disubstituted ferrocenes has been investigated by Mongin using mixed lithium–zinc bases for the deprotonative metalation of substituted ferrocenes containing a chiral directing group such as *N,N*-diisopropylcarboxamide (**73**).¹⁰⁶ By incorporating bis[(*S*)-1-phenylethyl] amino [(*S*)-PEA] into lithium amido/alkylzincates or dilithium diamido/dialkylzincates, S_p -product **74** was isolated as the major enantiomer after subsequent iodolysis. Conversely, the (*R_p*)-**74** enantiomer was favored after treatment of **73** with the monometallic lithium amide (*S*)-PEALi in the presence of metal salts. In particular, (*R_p*)-**74** was obtained with very high ee (96%), but with low yield (9%) with $CoBr_2$, whereas $ZnCl_2$ and $CdCl_2$ only gave 27 and 30% ee, respectively, but in excellent yields (94–96%). The best results in terms of yield and enantioselectivity *en route* to (*S_p*)-**74** were achieved using higher-order zincates such as $Me_2[(S)\text{-PEA}]_2ZnLi_2$ (99% yield; 65% ee) and $Et_2[(S)\text{-PEA}]_2ZnLi_2$ (97% yield 69% ee). A further screening of the reaction parameters led to the isolation of (*S_p*)-**74** in 97% yield and 86% ee after (i) 2 h reaction time at 0 °C, and (ii) by increasing the amount of $Me_2[(S)\text{-PEA}]_2ZnLi_2$ up to 2 equiv. (Scheme 25). A systematic study using chiral lithium zincates finally showed that higher-order zincates indeed displayed higher reactivity in the synthesis of **74** at lower temperature (about 90% yield at –20 °C) than lower-order lithium zincates (55–60% yield), with **74** being isolated with 96% yield and 86% ee when using 2 equiv. of $Me_2[(S)\text{-PEA}]_2ZnLi_2$, at 0 °C in THF, but with a contact time between the zincate base and **73** of only 0.5 h (Scheme 25).¹⁰⁷



Scheme 25 Metalation of **73** using mixed PEA-based lithium-metal combinations or Me₂(PEA)₂ZnLi₂, followed by iodolysis, to give products (R_p)-**74** or (S_p)-**74**, respectively. RT=room temperature.

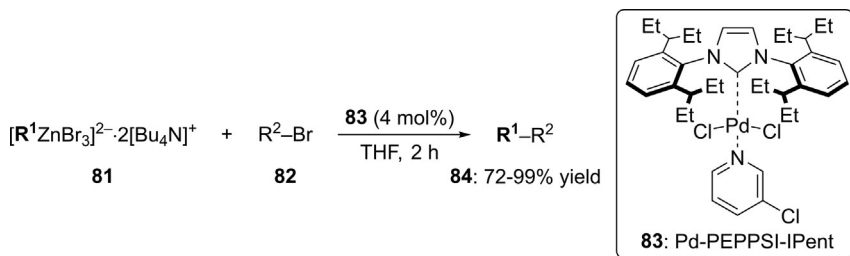
Oxidative coupling reactions using zincates derived from various bromoarenes and Me₄ZnLi₂ have been reported by Hirao.¹⁰⁸ The reaction between bromoarenes **75** (*ortho*-substituted bromoarenes, bromonaphthalene and bromoanthracene) and Me₄ZnLi₂ proceeded smoothly (in THF at 0 °C for 2 h) to yield methylated arenes **77** in good yields (51–99%) after treatment with VO(OEt)Cl₂, in order to oxidize the putative aryltrimethylzincate intermediate **76** (Scheme 26A). The reaction is proposed to proceed *via* one-electron oxidation between the organozincate complex and the oxovanadium(V) compound, or *via* transmetalation. Aside from coupling reactions between *sp*³ and *sp*² carbon centers, the combination Me₄ZnLi₂/VO(OEt)Cl₂ proved to be synthetically useful for achieving stereoselectively methyl-substituted cyclopropanes **80** starting from *gem*-dibromocyclopropane derivatives **78** *via* the putative trimethylzincate **79** at –78 °C (Scheme 26B).



Scheme 26 Methylation of (A) bromoarenes **75** and (B) *gem*-dibromocyclopropane **78** *via* oxovanadium(V)-induced oxidative ligand coupling reactions with Me₄ZnLi₂.

The first direct involvement of higher-order zincates in alkyl-alkyl Negishi cross-coupling reactions has been provided by Organ.¹⁰⁹ It was found that the tetrabutylammonium zincate **81**, in the absence of any salt additive, cross-coupled very quickly and cleanly with aryl bromides **82**

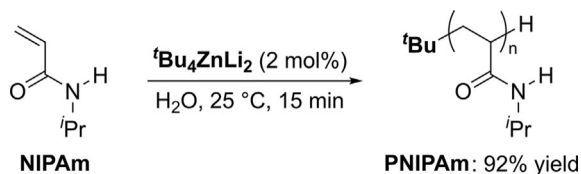
in THF when using Pd-PEPPSI-IPent (**83**) as the catalyst to afford Csp^3-Csp^3 products **84** in 72–99% yield (Scheme 27). Interestingly, it was also ascertained that the “ate” complex **81**, easily prepared by mixing the appropriate dialkylzinc with $[Bu_4N]Br$, is the active species undergoing transmetalation (which is the rate-determining step), thus completing the catalytic cycle. At the same time, the strong coordination ability of a polar solvent like THF was proven to play a major role in promoting the formation of such higher-order zincates by stabilizing them. Indeed, cross-couplings involving classical dialkyl reagents did not proceed without a polar solvent even in the presence of MX_n additives (e.g., LiCl, MBr_2).



Scheme 27 Pd-catalyzed alkyl-alkyl Negishi cross-coupling between preformed tetrabutylammonium zincates **81** and alkyl bromides **82** in THF to give products **84**.

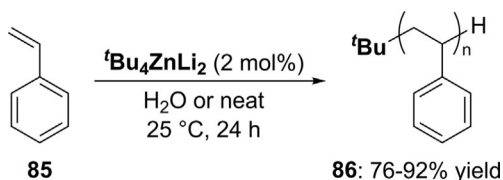
3.3 Polymerization reactions

Uchiyama first reported the use of tetra-*tert*-butylzincate $[tBu_4ZnLi_2]$, possessing high nucleophilicity for 1,4-addition reactions but weak basicity, as an initiator to trigger the chemoselective anionic polymerization of multifunctionalized monomers, such as *N*-isopropylacrylamide (NIPAm), *N,N*-dimethylacrylamide, acrylamide, and 2-hydroxyethyl methylacrylate.¹¹⁰ When using protic polar solvents such as MeOH and H_2O , such anionic polymerization reactions proved to be dramatically accelerated when compared to aprotic, less polar solvents. In H_2O , in particular, the yield of PNIPAm reached the maximum (92%) after just 15 min reaction time (Scheme 28). The polymer growth was well-regulated and the terminal zincate of the polymer chain could even be further decorated by trapping reactions with electrophiles to afford highly functionalised macromolecules. Contrastingly, the polymerization reactions when using methyl-zincates (e.g., Me_3ZnLi or Me_4ZnLi_2) as initiators did not proceed at all.



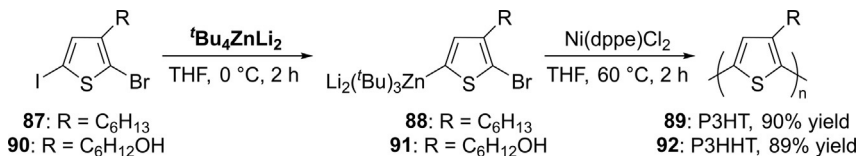
Scheme 28 Organozincate-mediated anionic polymerization of NIPAm in H₂O at room temperature to give PNIPAm.

In contrast to PNIPAm, polymerization of styrene **85** (which is not activated by a conjugate carbonyl group like acryl acid derivatives) with ^tBu₄ZnLi₂ proceeded smoothly at room temperature in an aprotic solvent (e.g., Et₂O) or under bulk polymerization conditions to give polystyrene **86** with low polydispersity (PDI) in 76–92% yield after 24 h (Scheme 29).⁹⁶ ¹H NMR data were consistent with linear structures, which strongly support an anionic polymerization process. Detailed spectroscopic and theoretical investigations on the structure of ^tBu₄ZnLi₂ also clarified that is this dianionic zincate and not ^tBu₃ZnLi which is the active species involved in THF solution and in the gas phase (see Section 2.3 for more details). The lower-order zincate [^tBu₃ZnLi], was found to be less stable than [^tBu₄ZnLi₂] and highly prone to undergo disproportionation to give [^tBu₂Zn] and [^tBu₄ZnLi₂] in THF solution.⁹⁶



Scheme 29 Anionic polymerization of styrene by using ^tBu₄ZnLi₂ as an initiator.

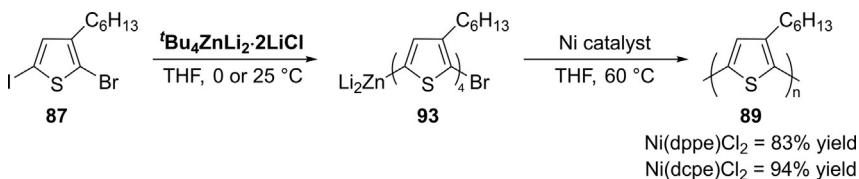
The halogen–metal exchange reaction of 2-bromo-3-hexyl-5-iodothiophene (**87**) with an equimolar amount of ^tBu₄ZnLi₂, followed by a Negishi-type catalyst-transfer polycondensation (NCTP) of the putative zincated monomer intermediate **88** using 1,3-bis(diphenylphosphino) ethanenickel dichloride [Ni(dppf)Cl₂] as the catalyst, paved the way for a high yielding (90%) synthesis of high-molecular weight (MW) (up to 30 kDa) regioregular poly(3-hexylthiophene) (P3HT) (**89**), which was characterized by low PDI (Scheme 30).¹¹¹ Interestingly, the aforementioned protocol could also be successfully applied (i) using as-received THF even in the presence of 1000 ppm water, and (ii) to synthesize poly[3-(6-hydroxyhexyl)thiophene] (P3HHT) (**92**) (89% yield) from the monomer



Scheme 30 Halogen-metal exchange reactions and catalyst-transfer polycondensation for the synthesis of P3HT (**89**) and P3HHT (**92**) using ^tBu₄ZnLi₂.

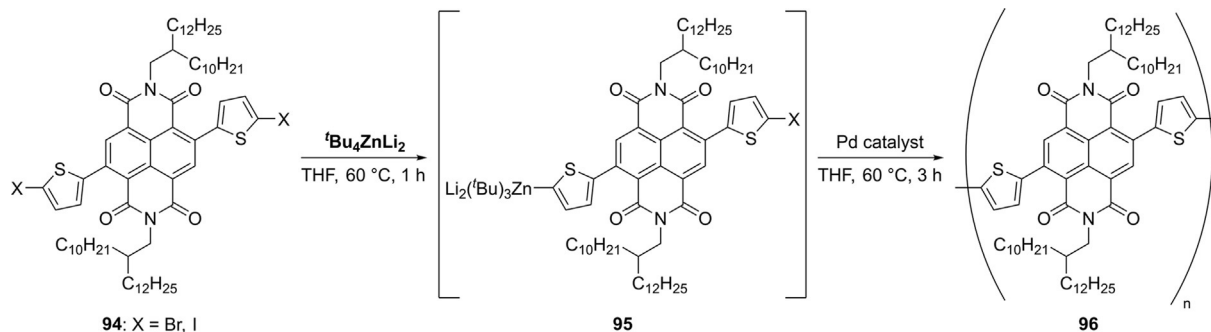
precursor **91**, in turn obtained from dihalogeno-derivative **90**, without any protection of the OH functional group (Scheme 30).¹¹¹

An environmentally responsible and atom-economical polymerization process was subsequently reported by Higashihara and Goto. By carefully investigating the stoichiometry in the zinc-iodine exchange reaction of **87** with both ^tBu₄ZnLi₂ and ^tBu₄ZnLi₂·2LiCl, they disclosed that the presence of LiCl strongly affected the structure of the zincated intermediate, and thus the following NCTP process. Of note, when the feed ratio between **87** and ^tBu₄ZnLi₂·2LiCl was calibrated to 1:0.25, the yield of the zinc-iodine exchange was quantitative and high-MW P3HT was obtained in a high yield (83%), presumably *via* the tetra-substituted monomer **93**. The changing of Ni(dppe)Cl₂ to 1,2-bis(dicyclohexylphosphanyl)ethane [Ni(dcpe)Cl₂], further improved the polymerization process, resulting in the formation of P3HT in 94% yield and with extremely low Đ value (1.04) (Scheme 31).¹¹²



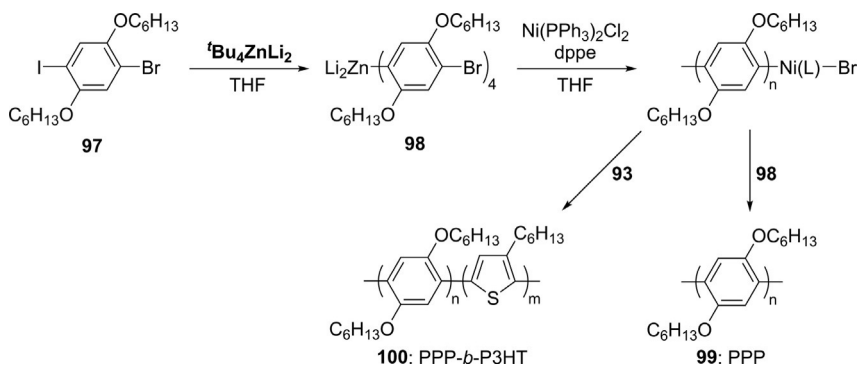
Scheme 31 Synthesis of P3HT (**89**) using 0.25 equiv. of ^tBu₄ZnLi₂·2LiCl with respect to **87** catalyzed by Ni(dppe)Cl₂ or Ni(dcpe)Cl₂ *via* the tetra-substituted monomer **93**.

Higashihara also investigated the NCTP of electron-deficient naphthalene-diimide containing monomers using ^tBu₄ZnLi₂ to synthesize electron-deficient *n*-type polymers. Zinc-halogen exchange reaction on the dihalogenated monomer precursor **94** was quantitatively carried out at 60 °C for 1 h without any protection of the imide group. Then, when a mixed solution of Pd₂(dba)₃ and P(*o*-Tolyl)₃ was employed, the electron-deficient polymer **96** was obtained with high MW (*M*_n = 8, 400) and a relatively low Đ (1.35) *via* the zincated monomer **95** (Scheme 32).¹¹³



Scheme 32 Synthesis of electron-deficient polymers **96** from electron-deficient monomers **94** via zincated monomer **95** using $\text{tBu}_4\text{ZnLi}_2$.

The NCTP method also proved to be effective to synthesize a variety of π -conjugated polymers. A well-defined poly(2,5-dihexyloxyphenylene-1,4-diyl) (PPP) (**99**) with controlled M_n (10900) and low \mathcal{D} (1.09) was successfully prepared using ${}^t\text{Bu}_4\text{ZnLi}_2$ (0.25 equiv. with respect to **97**) in combination with $\text{Ni}(\text{PPh}_3)_2\text{Cl}_2/\text{dppe}$ in THF at 60 °C for 1 h (Scheme 33).¹¹⁴ The MW of PPP could be modulated by changing the feed ratio of the zincated monomer (**98**) and Ni catalyst, while maintaining a low \mathcal{D} . Furthermore, in order to confirm the feasibility of chain extension between different monomers and the quasi-living end of NCTP, the block copolymer PPP-*b*-P3HT ($M_n = 132,600$, $\mathcal{D} = 1.15$) (**100**) was also satisfactorily prepared by the sequential addition of phenylene and thiophene monomers (**93**), using ${}^t\text{Bu}_4\text{ZnLi}_2$.



Scheme 33 Synthesis of PPP (**99**) and PPP-*b*-P3HT (**100**) by NCTP using ${}^t\text{Bu}_4\text{ZnLi}_2$.

4. Conclusions and outlook

While lithium zincates may have initially been considered mere curiosities in organometallic chemistry, over the last decade, these bimetallic reagents have emerged as a powerful and versatile family of heterobimetallic reagents, capable of promoting cornerstone organic transformations, which are out of the reach for conventional neutral organozinc reagents. By switching on chemical cooperativity, these systems can display enhanced reactivities and unique regioselectivities that cannot be replicated by their homometallic counterparts. Among these types of reagents tetraorgano-lithium zincates R_4ZnLi_2 ($\text{R} = \text{alkyl, alkenyl, allyl, aryl, alkynyl, etc.}$) have demonstrated a greater level of kinetic activation which ultimately leads to a stronger nucleophilic power. In parallel with these synthetic organic studies,

isolation, and structural elucidation of these heterobimetallic complexes have shed light on their constitution and the coordination preferences of lithium and zinc within zincate frameworks. Thus, in all the examples of higher-order zincates described in this chapter, the foundation of their structure is provided by four anchoring σ -based Zn—C bonds, as they comprise the stronger, more covalent interactions, with Zn adopting a distorted tetrahedral geometry. Contrastingly, the lithium ions affix to these frameworks *via* ancillary bonds to give contacted ion pairs, attaining further coordinative saturation, in most cases, by coordinating to a Lewis donor like TMEDA or THF. Complementing these structural studies, investigations on the constitution of these bimetallic compounds in solution using NMR spectroscopic techniques, in combination with theoretical calculations, have been performed. These studies have revealed that, depending on the Lewis donor employed and on the nature of the carbanionic substituents, higher- and lower order zincates can be formed and be in equilibrium with each other in solution. The presence of these equilibria with concomitant *in situ* generation of ZnR_2 or LiR can have important implications when assessing the reactivity of R_3ZnLi and R_4ZnLi_2 complexes. In this regard, hinting at an important alkali-metal effect, when assessing the stability and constitution of $[\text{Et}_4\text{ZnLi}_2]$. Thus, while this higher-order zincate is stable in solution in the presence of bidentate Lewis donors such as TMEDA or TMCDA, on the addition of the macrocyclic donor 12-crown-4, elimination of EtLi is observed yielding instead the lower order zincate $[\text{Et}_3\text{Zn}]^-\text{[Li(12-crown-4)}_2]^+$. While these findings seem to indicate that for this specific system higher-order zincates exhibiting a solvent-separated ion pair structure are not favored, further work is needed in terms of establishing this behavior as a general trend as well as investigating alkali-metal effects by replacing lithium by heavier alkali-metals.

As for the applications in organic synthesis, lithium tetraorganozincates (both homo- and heteroleptic compounds) were often found to exhibit higher reactivity and a singular chemo/regioselectivity toward either the halogen(tellurium)-zinc exchange or the nucleophilic addition and substitution reactions when compared to triorganozincates and organolithiums, even in the presence of acidic protons (e.g., phenolic OH, amide NH, glycerol C2-OH). The use of donor additives (e.g., TMEDA, HMPA) as well as electronic factors in the substrate contribute to modulate their reactivity/regioselectivity by influencing the structure and aggregation of these reagents in solution and privileging (if any) the formation of contacted ion pairs. However, transition-metal-catalyst- and ligand-free direct

arylation of aromatics (e.g., acridine) and alkylation/arylation of nitroolefins, β -nitroacrylates and β -nitroenones are also feasible and effective when using lithium tetraorganozincates, and take place with high chemoselectivity. The observation that either polar solvents like THF or protic polar solvents like MeOH and H₂O are required for the “stabilization” and the involvement of higher-order zincates in Negishi-like cross-coupling reactions, and as initiators to trigger chemoselective anionic polymerization of multifunctionalised monomers, paves the way for setting up more environmentally responsible processes with these unique, selective nucleophilic reagents, for example, by using bio-based solvents, working under aerobic conditions, and hopefully also employing non-noble metals as catalysts.^{115–117} Finally, the fact that the incorporation of chiral nonracemic alkoxides or amines into the structure of higher-order zincates has been proven to promote the desymmetrisation of diarylsulfoxides and the asymmetric deprotonative metalation reactions in ferrocenes is quite promising for developing novel asymmetric catalytic transformations or kinetic resolution models.

Acknowledgments

V.C. and M.D. acknowledge MUR and CNR-IC for a fellowship within the framework of the National PRIN project “Unlocking Sustainable Technologies Through Nature-Inspired Solvents” (Code: 2017A5HXFC_002). A.M.B. and E.H. thank Universität Bern for generous financial support.

References

1. Frankland E. *Philos Trans R Soc Lond.* 1852;142:417–444.
2. Frankland E. *Philos Trans R Soc Lond.* 1855;145:259–275.
3. Seyferth D. *Organometallics.* 2001;20:2940–2955.
4. Wanklyn JA. *Proc R Soc London.* 1859;9:341–345.
5. Hurd DT. *J Org Chem.* 1948;13:711–713.
6. Wittig G. *Angew Chem Int Ed.* 1958;70:65–71.
7. Uchiyama M, Kameda M, Mishima O, et al. *J Am Chem Soc.* 1998;120:4934–4946.
8. Wheatley AEH. *New J Chem.* 2004;28:435–443.
9. Mulvey RE. *Organometallics.* 2006;25:1060–1075.
10. Robertson SD, Uzelac M, Mulvey RE. *Chem Rev.* 2019;119:8332–8405.
11. Mulvey RE, Mongin F, Uchiyama M, Kondo Y. *Angew Chem Int Ed.* 2007;46:3802–3824.
12. Hirano K, Uchiyama M. *Polar Organometallic Reagents.* Wiley; 2022:337–364.
13. Fazekas E, Lowy PA, Abdul Rahman M, J. A. Garden. In: *Comprehensive Organometallic Chemistry IV.* Elsevier; 2022:193–304.
14. Uchiyama M, Furuyama T, Kobayashi M, Matsumoto Y, Tanaka K. *J Am Chem Soc.* 2006;128:8404–8405.
15. Merkel S, Stern D, Henn J, Stalke D. *Angew Chem Int Ed.* 2009;48:6350–6353.
16. Armstrong DR, Emerson HS, Hernán-Gómez A, Kennedy AR, Hevia E. *Dalton Trans.* 2014;43:14229–14238.

17. Uchiyama M, Matsumoto Y, Nobuto D, Furuyama T, Yamaguchi K, Morokuma K. *J Am Chem Soc.* 2006;128:8748–8750.
18. Clegg W, Dale SH, Hevia E, Honeyman GW, Mulvey RE. *Angew Chem Int Ed.* 2006;45:2370–2374.
19. Balkenhohl M, Ziegler DS, Desaintjean A, et al. *Angew Chem Int Ed.* 2019;58:12898–12902.
20. Redshaw C, Elsegood MRJ. *Chem Commun.* 2006;150:523–525.
21. Williams CK, White AJP. *J Organomet Chem.* 2007;692:912–916.
22. Jana S, Aksu Y, Driess M. *Dalton Trans.* 2009;1516–1521.
23. Clegg W, Graham DV, Herd E, et al. *Inorg Chem.* 2009;48:5320–5327.
24. Graham DV, Hevia E, Kennedy AR, Mulvey RE. *Organometallics.* 2006;25:3297–3300.
25. Woodruff D, Bodensteiner M, Sells DO, Winpenny REP, Layfield RA. *Dalton Trans.* 2011;40:10918–10923.
26. Boss SR, Coles MP, Eyre-Brook V, et al. *J Chem Soc Dalton Trans.* 2006;799:5574–5582.
27. Davies RP, Linton DJ, Snaith R, Wheatley AEH. *Chem Commun.* 2000;3:1819–1820.
28. Guo Z, Wang Y, Cao W, Chao J, Wei X. *Dalton Trans.* 2017;46:2765–2769.
29. Marciniak W, Merz K, Moreno M, Driess M. *Organometallics.* 2006;25:4931–4933.
30. Bond AD, Linton DJ, Schooler P, Wheatley AEH. *J Chem Soc Dalton Trans.* 2001;3173–3178.
31. Wang Y, Xie Y, Abraham MY, et al. *Angew Chem Int Ed.* 2012;51:10173–10176.
32. Cole ML, Evans DJ, Junk PC, Louis LM. *New J Chem.* 2002;26:1015–1024.
33. Hitchcock PB, Lappert MF, Wei XH. *J Chem Soc Dalton Trans.* 2006;60:11811181–11871187.
34. Redshaw C, Jana S, Shang C, Elsegood MRJ, Lu X, Guo ZX. *Chem Commun.* 2010;46:9055.
35. Davies RP, Linton DJ, Schooler P, Snaith R, Wheatley AEH. *Chem A Eur J.* 2001;7:3696–3704.
36. Su Y, Zhao Y, Gao J, Dong Q, Wu B, Yang XJ. *Inorg Chem.* 2012;51:5889–5896.
37. Kajiwara T, Terabayashi T, Yamashita M, Nozaki K. *Angew Chem Int Ed.* 2008;47:6606–6610.
38. Varonka MS, Warren TH. *Inorg Chim Acta.* 2007;360:317–328.
39. Schmidt S, Schulz S, Bläser D, Boese R, Bolte M. *Organometallics.* 2010;29:6097–6103.
40. Azarifar D, Coles MP, El-Hamruni SM, Eaborn C, Hitchcock PB, Smith JD. *J Organomet Chem.* 2004;689:1718–1722.
41. Eisenmann T, Khanderi J, Schulz S, Flörke U. *Z Anorg Allg Chem.* 2008;634:507–513.
42. Prust J, Hohmeister H, Stasch A, et al. *Eur J Inorg Chem.* 2002;2:2156–2162.
43. Prust J., Most K, Stasch A, Roesky HW, Uson I. *Eur J Inorg Chem.* 2001;1613–1616.
44. Wang Y, Quillian B, Wannere GS, Wei P, von R. Schleyer P, Robinson GH. *Organometallics.* 2007;26:3054–3056.
45. Nguyen MT, Gabidullin B, Nikonov GI. *Dalton Trans.* 2018;47:4607–4612.
46. Hernán-Gómez A, Herd E, Hevia E, et al. *Angew Chem Int Ed.* 2014;53:2706–2710.
47. Leung W, Ip QW, Lam T, Mak TCW. *Organometallics.* 2004;23:1284–1291.
48. Liu J, Vieille-Petit L, Linden A, Luan X, Dorta R. *J Organomet Chem.* 2012;719:80–86.
49. Hitchcock PB, Huang Q, Lappert MF, Zhou M. *Dalton Trans.* 2005;2988.
50. Blake AJ, Gillibrand NL, Moxey GJ, Kays DL. *Inorg Chem.* 2009;48:10837–10844.
51. Jones C, Furness L, Nembenna S, Rose RP, Aldridge S, Stasch A. *Dalton Trans.* 2010;39:8788–8795.
52. Jones C, Junk PC, Steed JW, Thomas RC, Williams TC. *J Chem Soc Dalton Trans.* 2001;3219–3226.

53. Hollingsworth TS, Hollingsworth RL, Rosen T, Groysman S. *RSC Adv.* 2017;7: 41819–41829.
54. Thiele K, Görls H, Seidel W. *Z Anorg Allg Chem.* 1998;624:555–556.
55. Dontha R, Zhu TC, Shen Y, Wörle M, Hong X, Duttwyler S. *Angew Chem Int Ed.* 2019;58:19007–19013.
56. Wang G, Dias HVR. *Eur J Inorg Chem.* 2017;2017:5507–5514.
57. Dobrovetsky R, Bravo-Zhivotovskii D, Tumanskii B, Botoshansky M, Apeloig Y. *Angew Chem Int Ed.* 2010;49:7086–7088.
58. Krasovskiy A, Knochel P. *Angew Chem Int Ed.* 2004;43:3333–3336.
59. Li-Yuan Bao R, Zhao R, Shi L. *Chem Commun.* 2015;51:6884–6900.
60. Krasovskiy A, Krasovskaya V, Knochel P. *Angew Chem Int Ed.* 2006;45:2958–2961.
61. Knochel P, ed. *Handbook of Functionalized Organometallics.* Wiley; 2005.
62. Eckert P, Sharif S, Organ MG. *Angew Chem Int Ed.* 2021;60:12224–12241.
63. Ochiai H, Jang M, Hirano K, Yorimitsu H, Oshima K. *Org Lett.* 2008;10:2681–2683.
64. McCann LC, Organ MG. *Angew Chem Int Ed.* 2014;53:4386–4389.
65. Krasovskiy A, Malakhov V, Gavryushin A, Knochel P. *Angew Chem Int Ed.* 2006;45: 6040–6044.
66. Koszinowski K, Böhler P. *Organometallics.* 2009;28:771–779.
67. Feng C, Cunningham DW, Easter QT, Blum SA. *J Am Chem Soc.* 2016;138: 11156–11159.
68. Jess K, Kitagawa K, Tagawa TKS, Blum SA. *J Am Chem Soc.* 2019;141:9879–9884.
69. Harrison-Marchand A, Mongin F. *Chem Rev.* 2013;113:7470–7562.
70. Weiss E. *Angew Chem Int Ed.* 1993;32:1501–1523.
71. Mongin F, Harrison-Marchand A. *Chem Rev.* 2013;113:7563–7727.
72. Gil-Negrete JM, Hevia E. *Chem Sci.* 2021;12:1982–1992.
73. Borys AM, Hevia E. *Trends Chem.* 2021;3:803–806.
74. Guo Y, Weiss R, Boese R, Epple M. *Thermochim Acta.* 2006;446:101–105.
75. Ponikvar W, Mayer P, Piotrowski H, Swoboda P, Oetker C-J, Beck W. *Z Anorg Allg Chem.* 2002;628:15–19.
76. Platten AWJ, Borys AM, Hevia E. *ChemCatChem.* 2022;14:2–7.
77. Edwards AJ, Fallaize A, Raithby PR, et al. *J Chem Soc Dalton Trans.* 1996;133.
78. Gao J, Li S, Zhao Y, Wu B, Yang XJ. *Organometallics.* 2012;31:2978–2985.
79. Weiss E, Wolftrum R. *Chem Ber.* 1968;101:35–40.
80. Armstrong DR, Dougan C, Graham DV, Hevia E, Kennedy AR. *Organometallics.* 2008;27:6063–6070.
81. Brien PO, Hursthouse MB, Jones AC, Motevalli M, Walsh JR. *J Organomet Chem.* 1993;449:1–8.
82. Bacsa J, Hanke F, Hindley S, et al. *Angew Chem Int Ed.* 2011;50:11685–11687.
83. Dell'Aera M, Perna FM, Vitale P, et al. *Chem A Eur J.* 2020;26:8742–8748.
84. Fröhlich HO, Kosan B, Müller B, Hiller W. *J Organomet Chem.* 1992;441:177–184.
85. Fröhlich HO, Kosan B, Undeutsch B, Görls H. *J Organomet Chem.* 1994;472:1–14.
86. Wyrwa R, Fröhlich HO, Görls H. *Organometallics.* 1996;15:2833–2835.
87. Zhang Y, Liu L, Chen T, Huang Z, Zhang WX, Xi Z. *Organometallics.* 2019;38: 2174–2178.
88. Rijnberg E, Jastrzebski JTBH, Boersma J, et al. *Organometallics.* 1997;16:2239–2245.
89. Clegg W, Conway B, Hevia E, McCall MD, Russo L, Mulvey RE. *J Am Chem Soc.* 2009;131:2375–2384.
90. Hernán-Gómez A, Herd E, Uzelac M, et al. *Organometallics.* 2015;34:2614–2623.
91. Roberts AJ, Kennedy AR, McLellan R, Robertson SD, Hevia E. *Eur J Inorg Chem.* 2016;2016:4752–4760.
92. Cremer U, Pantenburg I, Ruschewitz U. *Inorg Chem.* 2003;42:7716–7718.

93. Cremer U, Ruschewitz U. *Z Anorg Allg Chem.* 2004;630:337–343.
94. De Tullio M, Borys AM, Hernán-Gómez A, Kennedy AR, Hevia E. *Chem Catal.* 2021;1:1308–1321.
95. Mobley TA, Berger S. *Angew Chem Int Ed.* 1999;38:3070–3072.
96. Furayama T, Yonehara M, Arimoto S, Kobayashi M, Matsumoto Y, Uchiyama M. *Chem A Eur J.* 2008;14:10348–10356.
97. Armstrong DR, Baillie SE, Blair VL, et al. *Chem Sci.* 2013;4:4259–4266.
98. Uchiyama M, Koike M, Kameda M, Kondo Y, Sakamoto T. *J Am Chem Soc.* 1996;118:8733–8734.
99. Chau NTT, Meyer M, Komagawa S, et al. *Chem A Eur J.* 2010;16:12425–12433.
100. Kato Y, Williams CM, Uchiyama M, Matsubara S. *Org Lett.* 2019;21:473–475.
101. Balkenhohl M, Knochel P. *Chem A Eur J.* 2020;26:3688–3697.
102. Hatano M, Ito O, Suzuki S, Ishihara K. *J Org Chem.* 2010;75:5008–5016.
103. Hatano M, Mizuno M, Ishihara K. *Org Lett.* 2016;18:4462–4465.
104. Nakamura S, Uchiyama M, Ohwada T. *J Am Chem Soc.* 2004;126:11146–11147.
105. Ruppenthal S, Brückner R. *Eur J Org Chem.* 2018;2018:2518–2530.
106. Dayaker G, Tilly D, Chevallier F, Hilmersson G, Gros PC, Mongin F. *Eur J Org Chem.* 2012;6051–6057.
107. Hedidi M, Dayaker G, Kitazawa Y, et al. *New J Chem.* 2019;43:14898–14907.
108. Takada T, Sakurai H, Hirao T. *J Org Chem.* 2001;66:300–302.
109. McCann LC, Hunter HN, Clyburne JAC, Organ MG. *Angew Chem Int Ed.* 2012;51:7024–7027.
110. Kobayashi M, Matsumoto Y, Uchiyama M, Ohwada T. *Macromolecules.* 2004;37:4339–4341.
111. Higashihara T, Goto E, Ueda M. *ACS Macro Lett.* 2012;1:167–170.
112. Goto E, Higashihara T. *Microsyst Technol.* 2016;22:39–44.
113. Goto E, Mori H, Ueda M, Higashihara T. *J Photopolym Sci Technol.* 2015;28:279–283.
114. Ochiai Y, Goto E, Higashihara T. *Macromol Rapid Commun.* 2017;38:2–5.
115. García-Álvarez J, Hevia E, Capriati V. *Chem A Eur J.* 2018;24:14854–14863.
116. Perna FM, Vitale P, Capriati V. *Curr Opin Green Sustain Chem.* 2021;30:100487.
117. García-Garrido SE, Presa Soto A, Hevia E, García-Álvarez J. *Eur J Inorg Chem.* 2021;31:3116–3160.